fractal and fractional

MDPI

Article

Fractional Dynamics of Typhoid Fever Transmission Models with Mass Vaccination Perspectives

Hamadjam Abboubakar [1,*], Raissa Kom Regonne [2,†] and Kottakkaran Sooppy Nisar [3,*,†]

[1] Department of Computer Engineering, University Institute of Technology of Ngaoundéré, University of Ngaoundéré, Ngaoundéré P.O. Box 455, Cameroon
[2] National School of Agro-Industrial Sciences, University of Ngaoundéré, Ngaoundéré P.O. Box 455, Cameroon; rkregonne@yahoo.fr
[3] Department of Mathematics, College of Arts and Science, Prince Sattam bin Abdulaziz University, Wadi Aldawaser 11991, Saudi Arabia
* Correspondence: h.abboubakar@gmail.com or hamadjam.abboubakar@univ-ndere.cm (H.A.); n.sooppy@psau.edu.sa (K.S.N.); Tel.: +237-694-52-3111 (H.A.)
† These authors contributed equally to this work.

Abstract: In this work, we formulate and mathematically study integer and fractional models of typhoid fever transmission dynamics. The models include vaccination as a control measure. After recalling some preliminary results for the integer model (determination of the epidemiological threshold denoted by $\mathcal{R}_c$, asymptotic stability of the equilibrium point without disease whenever $\mathcal{R}_c < 1$, the existence of an equilibrium point with disease whenever $\mathcal{R}_c > 1$), we replace the integer derivative with the Caputo derivative. We perform a stability analysis of the disease-free equilibrium and prove the existence and uniqueness of the solution of the fractional model using fixed point theory. We construct the numerical scheme and prove its stability. Simulation results show that when the fractional-order η decreases, the peak of infected humans is delayed. To reduce the proliferation of the disease, mass vaccination combined with environmental sanitation is recommended. We then extend the previous model by replacing the mass action incidences with standard incidences. We compute the corresponding epidemiological threshold denoted by $\mathcal{R}_{c\star}$ and ensure the uniform stability of the disease-free equilibrium, for both new models, when $\mathcal{R}_{c\star} < 1$. A new calibration of the new model is conducted with real data of Mbandjock, Cameroon, to estimate $\mathcal{R}_{c\star} = 1.4348$. We finally perform several numerical simulations that permit us to conclude that such diseases can possibly be tackled through vaccination combined with environmental sanitation.

Keywords: typhoid fever disease; vaccination; model calibration; Caputo derivative; asymptotic stability; fixed point theory

MSC: 26A33; 93D20; 47H10; 93E24; 92D30

Citation: Abboubakar, H.; Kom Regonne, R.; Sooppy Nisar, K. Fractional Dynamics of Typhoid Fever Transmission Models with Mass Vaccination Perspectives. *Fractal Fract.* **2021**, *5*, 149. https://doi.org/10.3390/fractalfract5040149

Academic Editor: Vasily E. Tarasov

Received: 7 August 2021
Accepted: 20 September 2021
Published: 30 September 2021

1. Introduction

Typhoid fever, caused by a salmonella bacterium (*Salmonella typhi*), is a tropical disease transmitted by the ingestion of food or/and water contaminated with feces. It is most prevalent in countries located below the equator, in Southeast Asia, and in the Indian subcontinent, where hygiene conditions are poor [1,2]. The principal symptoms of typhoid fever are insomnia, fever, generalized fatigue, headaches, stomach ache, anorexia, constipation or diarrhea, and vomiting. These symptoms can last several weeks. Without effective treatment, typhoid fever can lead to death. According to the World Health Organization (WHO), the number of cases of typhoid fever is estimated to be between 11 and 21 million, with 128,000 to 161,000 deaths annually due to the severity of the disease [1,2]. Vaccination, sanitary measures, and hygiene measures are the best ways to prevent the spread of the disease [2].

Since the work of Sir Ronald Ross on malaria [3], mathematical tools such as differential equations have usually been used to understand and describe the dynamics of infectious diseases [4–12]. In [7], the authors proposed a $SVII_cR$ that takes into account some control mechanisms (treatment, education campaigns, and vaccination). Quarantining the infected individuals and their treatment are the main control measures studied in [8]. The author used optimal control methods to conclude that the outbreak can be eliminated or controlled if the control strategies are combined to their highest levels. The same conclusions are given in [10,11]. Recently, Olumuyiwa James et al. [9] formulated and studied an optimal control model for typhoid fever that takes into account both indirect and direct transmission. They compared various proposed strategies using numerical simulations and concluded that the disease burden can be controlled if all the available control measures are combined.

Very recently, many authors have proposed fractional-order models in mathematical epidemiology (ref. [13]), ecology (ref. [14]), plant epidemiology (refs. [15,16]), and psychology (ref. [17]). Indeed, the necessity of the use of fractional derivatives in epidemiology, for example, comes from the fact that these operators have many properties, such as their different types of kernels and the crossover behavior in the model, which can only be described using these operators. Moreover, any real data that have zigzag dynamics (mostly many) that cannot be projected by an integer-order derivative can be solved by a fractional model more clearly.

The principal disadvantage of models with integer derivatives is that they do not permit the definition of memory effects. Replacing integer derivatives with fractional derivatives makes it possible to remedy this problem. Indeed, they offer different ways to forecast data by varying the fractional-order parameter [12,18,19]. Several fractional operators have been defined so far. The most popular are the fractional operators of Caputo, the fractional Caputo–Fabrizio operator, and the fractional operator of Atangana–Baleanu. Each operator explores the dynamics of the studied phenomenon differently, thus helping us to predict more variations in the evolution of the phenomenon. The advantages and disadvantages of each fractional operator and their application domains can be found in [20–22].

To the best of our knowledge, there are few mathematical works on typhoid fever using fractional operators [6,12]. In [12], the authors used the Caputo–Fabrizio operator to extend the model proposed in [23]. They provided existence, uniqueness, and stability criteria for the proposed fractional-order typhoid model. More recently, Abboubakar et al. [6] formulated a SIR-B-type compartmental model with both integer and Caputo derivatives. The only control measure was vaccination. They computed the control reproduction number, R_c, and performed stability analysis of the disease-free equilibrium point for both models. The present contributions are listed as follows:

1. Using a fractional derivative in place of an integer derivative, as used in our previous model [5], we formulate a new model. To prove the existence and uniqueness of the solutions, we use fixed point theory. The corresponding numerical scheme is obtained through the Adams–Bashforth–Moulton method [24,25]. The stability of this numerical scheme is also proven. Finally, several numerical simulations are carried out from the real values of parameters estimated with real data of Mbandjock, in Cameroon (see [5]).
2. Secondly, we extend the previous models by replacing the mass action incidence law with the standard incidence law. For these new models, we compute the corresponding control reproduction number, $\mathcal{R}_{c\star}$, and ensure the uniform stability of the equilibrium point without disease. As in [6], model parameters are estimated. With these new parameter values, we finally perform several numerical simulations that permit us to compare the quantitative dynamics of the two types of models.

The rest of the work is organized as follows. We devote Section 2 to preliminary definitions of the fractional derivative in the sense of Caputo and useful results. Formulation of the models with mass incidence law and standard incidence, as well as their mathematical

analysis (computation of control reproduction numbers, asymptotic stability analysis of the disease-free equilibrium, existence as well as the uniqueness of solutions, construction of the numerical scheme with its stability), is also described in this section. The calibration of the model with standard incidences and several numerical results is given in Section 3. We end the paper with a discussion and conclusions.

2. Materials and Methods

2.1. Useful Definitions and Results

For over ten years, fractional derivatives have captured the attention of researchers, who use these fractional operators to model physical, chemical, and biological processes. One can cite the dynamics of transmissible diseases [26–28]. Before the formulation of the fractional models, it is important to recall their definition, as well as two results that will be used later in the fractional model analysis.

Definition 1. *Let $f \in C^{l}_{-1}$, and we have the following relation:*

$$D^{\nu}_{\tau} f(\tau) = \begin{cases} \frac{d^{r} f(\tau)}{d\tau^{r}}, & \nu = r \in \mathbb{N} \\ \frac{1}{\Gamma(r-\nu)} \int_{0}^{\tau} (\tau - \iota)^{r-\nu-1} f^{(r)}(\iota) d\iota, & -1 + r < \nu < r, r \in \mathbb{N}, \end{cases} \tag{1}$$

which represents the Caputo derivative of f.

Lemma 1. *Assume that $\chi, \mathbf{Q}, \mathbf{h}, \mathbf{Y} > 0$, $\mathbf{kh} \leq \mathbf{Y}$ with $\mathbf{k} \in \mathbb{N}$, and*

$$\mathbf{y}_{q,m} = \begin{cases} (m-q)^{\chi-1} & q = 1, 2, \ldots, m-1, \\ 0 & q \geq m. \end{cases}$$

Let $\sum_{q=\mathbf{k}}^{q=i} \mathbf{y}_{q,m} |\mathbf{e}_q| = 0$ for $\mathbf{k} > m \geq 1$.
If

$$|\mathbf{e}_m| \leq \mathbf{Q}\mathbf{h}^{\chi} \sum_{q=1}^{m-1} \mathbf{y}_{q,m} |\mathbf{e}_q| + |\eta_0|, \quad m = 1, 2, \ldots, \mathbf{k},$$

then

$$|\mathbf{e}_k| \leq \mathcal{M} |\eta_0|, \quad \mathbf{k} \in \{1, 2, \ldots\}$$

where $\mathcal{M} \in \mathbb{R}_{+}$ does not depend on $\mathbf{h}$ and $\mathbf{k}$.

Lemma 2. *If $0 < \chi < 1$ and $\mathbf{d} \in \mathbb{N}$, then there exist positive constants $W_{\chi,1}$ and $W_{\chi,2}$ only dependent on χ, such that*

$$(1+\mathbf{v})^{\chi} - \mathbf{v}^{\chi} \leq \mathcal{W}_{\chi,1} (1+\mathbf{v})^{\chi-1} \quad \text{and} \quad (2+\mathbf{v})^{\chi+1} - 2(1+\mathbf{v})^{\chi+1} + \mathbf{v}^{\chi+1} \leq \mathcal{W}_{\chi,2} (1+\mathbf{v})^{\chi-1}.$$

2.2. Model Dynamics with Mass Action Incidence Law

2.2.1. Model Formulation in ODE Sense and Its Analysis

In a previous work [5], we formulated and analyzed a new mathematical model for the transmission dynamics of typhoid fever with application to the town of Mbandjock, in the central region of Cameroon. The model is divided into seven compartments: susceptible individuals $S(t)$, vaccinated individuals $V(t)$, infected individuals in latent stage $E(t)$, infected individuals without any sign of the disease $C(t)$, symptomatic infected individuals $I(t)$, recovered individuals $R(t)$, and the density of bacteria in the environment $B(t)$. Each individual in each compartment naturally dies at a rate μ_h. Susceptible humans are recruited at a constant rate Λ_h. The population in compartment S_h decreases either by vaccination at a rate ξ, or by infection at an incidence rate $\nu B(t) S(t)$, where ν is the contact rate. We denote by θ the rate at which vaccinated individuals lose their immunity. The vaccine efficacy is denoted by ϵ. The compartment E of latent individuals, which include infected susceptible individuals and vaccinated individuals, progresses either to

the carriers compartment C at a rate $q\gamma_1$ or to the compartment I at the rate $(1-q)\gamma_1$. Asymptomatic individuals become symptomatic at the rate $(1-p)\gamma_2$ or recover at the rate $p\gamma_2$. δ denotes the disease-induced death rate of symptomatic individuals. Recovered individuals become susceptible at a rate α. With this brief description, the mathematical formulation of the model studied in [5] is presented as follows:

$$\dot{S}(t) = \Lambda_h - (k_1 + \nu B(t))S(t) + \theta V(t) + \alpha R(t), \tag{2a}$$
$$\dot{V}(t) = -[k_2 + (1-\epsilon)\nu B(t)]V(t) + \xi S(t), \tag{2b}$$
$$\dot{E}(t) = -k_3 E(t) + \nu[\pi V(t) + S(t)]B(t), \tag{2c}$$
$$\dot{C}(t) = q\gamma_1 E(t) - k_4 C(t), \tag{2d}$$
$$\dot{I}(t) = q_1\gamma_1 E(t) + p_1\gamma_2 C(t) - [k_5 + \sigma]I(t), \tag{2e}$$
$$\dot{R}(t) = p\gamma_2 C(t) + \sigma I(t) - k_6 R(t), \tag{2f}$$
$$\dot{B}(t) = p_c C(t) + p_i I(t) - \mu_b B(t), \tag{2g}$$

where $k_1 = \xi + \mu_h$, $k_2 = \theta + \mu_h$, $k_3 = \gamma_1 + \mu_h$, $k_4 = \mu_h + \gamma_2$, $k_5 = \delta + \mu_h$, $k_6 = \alpha + \mu_h$, $\pi = -1 + \epsilon$, $q_1 = 1 - q$, $p_1 = -p + 1$, $k_7 = k_1 k_2 - \theta\xi = \mu_h(k_2 + \xi) > 0$, $k_8 = k_5 + \sigma$.

Model (2) is defined in the following set:

$$\mathcal{W} = \left\{ (S, V, E, C, I, R, B)' \in \mathbb{R}_+^7 : N = V + S + C + E + I + R \leq \frac{\Lambda_h}{\mu_h}; B \leq \frac{(p_i + p_c)\Lambda_h}{\mu_h \mu_b} \right\},$$

in which a dynamical system is defined, and where N denotes the human population.

Without disease, model (2) has the following equilibrium: $\mathcal{Q}_0 = (S_0, V_0, 0, 0, 0, 0, 0)'$, where $S_0 = \Lambda_h k_2/(\mu_h(k_2 + \xi))$ and $V_0 = \Lambda_h \xi/(\mu_h(k_2 + \xi))$. Using the same approach developed in [29], we obtain the control reproduction number given by

$$\mathcal{R}_c = \sqrt{\frac{\nu\Lambda_h(k_2 + \pi\xi)\gamma_1[p_c q(\sigma + k_5) + p_i(k_4(1-q) + \gamma_2 q(1-p))]}{\mu_b \mu_h k_3 k_4 (k_2 + \xi)(\sigma + k_5)}}. \tag{3}$$

Considering the model without vaccination, R_c is equal to the basic reproduction number:

$$\mathcal{R}_0 = \sqrt{\frac{\nu\Lambda_h\gamma_1[p_c q(\sigma + k_5) + p_i(k_4(1-q) + \gamma_2 q(1-p))]}{\mu_b \mu_h k_3 k_4 (\sigma + k_5)}}. \tag{4}$$

Thus, it follows that

$$\mathcal{R}_c = \mathcal{R}_0 \sqrt{\frac{(k_2 + \pi\xi)}{(k_2 + \xi)}}.$$

Since $\pi\xi = (1-\epsilon)\xi \leq \xi$, we have $\dfrac{(k_2 + \pi\xi)}{(k_2 + \xi)} \leq 1$, which means that $\mathcal{R}_c \leq \mathcal{R}_0$. This proves that mass vaccination is a useful tool that can be used to effectively tackle this kind of tropical disease.

For typhoid model (2) in the ODE sense, the following results were proven in [5].

Proposition 1 ([5]). *For model (2), $\mathcal{Q}_0$ is locally and globally asymptotically stable in $\mathcal{W}$ if $\mathcal{R}_c < 1$ and unstable if $\mathcal{R}_c > 1$.*

Proposition 2 ([5]). *Let us define the following coefficients:*

$$\begin{aligned}
\mathbf{a}_2 &= \mathcal{R}_c^4 k_3^2 k_4^2 k_8^2 \mu_h^2 (\xi + k_2)^2 \pi \times \\
&\quad \times (\mu_h \gamma_1 \alpha (k_5 + \sigma q) + \gamma_2 \mu_h k_8 (\alpha + \gamma_1) + \gamma_1 \gamma_2 \alpha (1 - pq) k_5 + [\mu_h^2 + (\alpha + \gamma_2 + \gamma_1)\mu_h] \mu_h k_8), \\
\mathbf{a}_1 &= -\mathcal{R}_c^2 k_3^2 k_4^2 k_8^2 \mu_h^2 (\xi + k_2)^2 \gamma_1 \Lambda_h k_6 \pi (k_4 q_1 + \gamma_2 p_1 q)(\mathcal{R}_c^2 - \mathcal{R}_b^2), \\
\mathbf{a}_0 &= -\gamma_1^2 \mu_h \Lambda_h^2 k_3 k_4 k_6 k_8 (k_4 q_1 + \gamma_2 p_1 q)^2 (\pi \xi + k_2)^2 (\xi + k_2)(\mathcal{R}_c^2 - 1).
\end{aligned}$$

Model (2) with the integer derivative either has (1) only one endemic equilibrium whenever ($\mathbf{a}_0 < 0 \Longleftrightarrow \mathcal{R}_c > 1$) or ($\mathbf{a}_1 < 0$ and $\mathbf{a}_0 = 0$ or $\mathbf{a}_1^2 - 4\mathbf{a}_2\mathbf{a}_0 = 0$), (2) two endemic equilibrium points if ($\mathbf{a}_0 > 0$ ($\mathcal{R}_c < 1$), $\mathbf{a}_1 < 0$ ($\mathcal{R}_c > \mathcal{R}_b$) and $a_1^2 - 4\mathbf{a}_2\mathbf{a}_0 > 0$), or (3) no equilibrium otherwise.

Theorem 1 ([5]). *Model (2) exhibits a supercritical bifurcation at $\mathcal{R}_c = 1$, which implies that whenever $\mathcal{R}_c > 1$, the endemic equilibrium is locally asymptotically stable.*

Remark 1. *Proposition 1 combined with Theorem 1 implies that Proposition 2 (iii) will never hold true for model (2). Thus, the condition $\mathcal{R}_c < 1$ is sufficient to eradicate the disease.*

2.2.2. Fractional-Order Typhoid Model

The following model is obtained when we replace the integer derivative operator in (2) with the non-integer operator in the Caputo sense.

$$\begin{aligned}
{}_{t_0}^{C}D_t^{\eta} S(t) &= \Lambda_h - (k_1 + \nu B(t))S(t) + \theta V(t) + \alpha R(t), && \text{(5a)} \\
{}_{t_0}^{C}D_t^{\eta} V(t) &= -[k_2 + (1 - \epsilon)\nu B(t)]V(t) + \xi S(t), && \text{(5b)} \\
{}_{t_0}^{C}D_t^{\eta} E(t) &= -k_3 E(t) + \nu[\pi V(t) + S(t)]B(t), && \text{(5c)} \\
{}_{t_0}^{C}D_t^{\eta} C(t) &= q\gamma_1 E(t) - k_4 C(t), && \text{(5d)} \\
{}_{t_0}^{C}D_t^{\eta} I(t) &= q_1\gamma_1 E(t) + p_1\gamma_2 C(t) - [k_5 + \sigma]I(t), && \text{(5e)} \\
{}_{t_0}^{C}D_t^{\eta} R(t) &= p\gamma_2 C(t) + \sigma I(t) - k_6 R(t), && \text{(5f)} \\
{}_{t_0}^{C}D_t^{\eta} B(t) &= p_c C(t) + p_i I(t) - \mu_b B(t). && \text{(5g)}
\end{aligned}$$

with $S(0) \geq 0$, $V(0) \geq 0$, $B(0) \geq 0$, $E(0) \geq 0$, $I(0) \geq 0$, $C(0) \geq 0$, and $R(0) \geq 0$.

Asymptotic Stability of the Disease-Free Equilibrium

Before investigating the stability of the disease-free equilibrium point, we consider the fractional-order system (5) as follows:

$$ {}_{t_0}^{C}D_t^{\eta} \mathbf{x}(t) = \mathcal{F}(\mathbf{x}(t)), \tag{6}$$

where $\mathbf{x}(\zeta) \in \mathbb{R}^7$, $\mathcal{F} \in \mathbb{R}^7 \times \mathbb{R}^7$, $0 < \eta < 1$. The characteristic equation of the matrix $\mathcal{F}$ evaluated at any equilibrium (see [30]) is given by

$$\det(s(\mathbf{I} - (1 - \eta)\mathcal{F}) - \eta\mathcal{F}) = 0. \tag{7}$$

For the fractional model (5), the asymptotic stability of $\mathcal{Q}_0$ is claimed in the following result.

Theorem 2. *The disease-free equilibrium $\mathcal{Q}_0$ is uniformly asymptotically stable if $\mathcal{R}_c < 1$, and unstable otherwise.*

Proof. The Jacobian matrix of system (5) evaluated at the disease–free equilibrium $\mathcal{Q}_0$ is given by

$$J(\mathcal{Q}_0) = \begin{pmatrix} -k_1 & \theta & 0 & 0 & 0 & \alpha & -\nu S_0 \\ \xi & -k_2 & 0 & 0 & 0 & 0 & -\nu\pi V_0 \\ 0 & 0 & -k_3 & 0 & 0 & 0 & \nu(S_0+\pi V_0) \\ 0 & 0 & q\gamma_1 & -k_4 & 0 & 0 & 0 \\ 0 & 0 & q_1\gamma_1 & p_1\gamma_2 & -(k_5+\sigma) & 0 & 0 \\ 0 & 0 & 0 & p\gamma_2 & \sigma & -k_6 & 0 \\ 0 & 0 & 0 & p_c & p_i & 0 & -\mu_b \end{pmatrix} = \begin{pmatrix} J_1 & J_2 \\ J_3 & J_4 \end{pmatrix},$$

where $J_1 = \begin{pmatrix} -k_1 & \theta \\ \xi & -k_2 \end{pmatrix}$, $J_2 = \begin{pmatrix} 0 & 0 & 0 & \alpha & -\nu S_0 \\ 0 & 0 & 0 & 0 & -\nu\pi V_0 \end{pmatrix}$, $J_3 = O_{\mathbb{R}^{5\times 2}}$, and

$$J_4 = \begin{pmatrix} -k_3 & 0 & 0 & 0 & \nu(S_0+\pi V_0) \\ q\gamma_1 & -k_4 & 0 & 0 & 0 \\ q_1\gamma_1 & p_1\gamma_2 & -(k_5+\sigma) & 0 & 0 \\ 0 & p\gamma_2 & \sigma & -k_6 & 0 \\ 0 & p_c & p_i & 0 & -\mu_b \end{pmatrix}.$$

The characteristic Equation (7) of the typhoid fractional model (5) becomes

$$\begin{cases} \det(s(\mathbf{I}_2 - (1-\eta)J_1) - \eta J_1) = 0 \\ \det(s(\mathbf{I}_5 - (1-\eta)J_4) - \eta J_4) = 0, \end{cases} \tag{8}$$

which is equivalent to

$$\begin{cases} a_2 s^2 + a_1 s + a_0 = 0, \\ \{s[(1-\eta)k_6 + 1] + k_6\eta\}\left(s^4 + \frac{A_1}{A_5}s^3 + \frac{A_2}{A_5}s^2 + \frac{A_3}{A_5}s + \frac{A_4}{A_5}\right) = 0, \end{cases} \tag{9}$$

where $a_2 = (1-\eta)^2 k_7 + (1-\eta)(k_1+k_2) + 1$, $a_1 = 2\eta(1-\eta)k_7 + \eta(k_1+k_2)$, $a_0 = \eta^2 k_7$,

$$\begin{aligned} A_5 &= \eta_1^3 k_3 k_4 k_8 \mu_b (\eta_1 k_9 + q_1 p_i + p_c q)(1-\mathcal{R}_c^2) \\ &\quad + \eta_1^3 \mu_b [k_3 k_8 (k_8 p_c q + p_1\gamma_2 p_i q) + k_3 k_4 (q_1 k_4 p_i + p_1\gamma_2 p_i q) + k_4 k_8 k_9] \\ &\quad + \eta_1^2 \mu_b (k_8 k_9 + k_4 k_9 + k_3 k_9) + \eta_1 k_9 \mu_b \\ &\quad + \Big(\Big(\Big(\eta_1^3 k_3 + \eta_1^2\Big)k_4 + \eta_1^2 k_3 + \eta_1\Big)k_8 + \Big(\eta_1^2 k_3 + \eta_1\Big)k_4 + \eta_1 k_3 + 1\Big)k_9, \end{aligned}$$

$$\begin{aligned} A_1 &= \Big\{4k_3 k_4 k_8 k_9 \mu_b \eta_1^3 \eta + 3\eta_1^2 k_3 k_8 \mu_b \eta q_1 k_4 p_i + 3\eta_1^2 \eta k_3 k_4 \mu_b k_8 p_c q\Big\}(1-R_c^2) \\ &\quad + 3\eta_1^2 \eta k_3 k_4 \mu_b (q_1 k_4 p_i + p_1\gamma_2 p_i q) + 3\eta_1^2 k_3 k_8 \mu_b \eta [k_8 p_c q + p_1\gamma_2 p_i q] \\ &\quad + 2\eta_1 k_4 k_9 \mu_b \eta + (2\eta_1 k_3 + 1)k_9 \mu_b \eta + 3\eta_1^2 k_4 k_8 k_9 \mu_b \eta + 2\eta_1 k_8 k_9 \mu_b \eta \\ &\quad + \Big(\Big(\Big(3\eta_1^2 k_3 + 2\eta_1\Big)k_4 + 2\eta_1 k_3 + 1\Big)k_8 + (2\eta_1 k_3 + 1)k_4 + k_3\Big)k_9\eta, \end{aligned}$$

$$\begin{aligned} A_2 &= \Big[6\eta_1^2 k_3 k_4 k_8 k_9 \mu_b \eta^2 + 3\eta_1 k_3 k_4 k_8 \mu_b \eta^2 (p_c q + q_1 p_i)\Big](1-\mathcal{R}_c^2) \\ &\quad + 3\eta_1 \eta^2 [k_3 k_8 \mu_b (k_8 p_c q + p_1\gamma_2 p_i q) + k_4 k_8 k_9 (\mu_b + k_3) + k_3 k_4 \mu_b (q_1 k_4 p_i + p_1\gamma_2 p_i q)] \\ &\quad + (k_4 k_8 + k_3 k_8 + k_3 k_4 + k_8 \mu_b + k_4 \mu_b + k_3 \mu_b) k_9 \eta^2, \end{aligned}$$

$$\begin{aligned} A_3 &= \mu_b \eta^3 k_3 k_4 k_8 [4k_9\eta_1 + q_1 p_i + p_c q](1-\mathcal{R}_c^2) \\ &\quad + (\mu_b + k_3) k_4 k_8 k_9 \eta^3 + k_3 \mu_b \eta^3 \{k_8 q (k_8 p_c + p_1\gamma_2 p_i) + k_4 p_i (q_1 k_4 + p_1\gamma_2 q)\}, \end{aligned}$$

$$A_4 = \Big(1-\mathcal{R}_c^2\Big)\eta^4 k_3 k_4 k_8 \mu_b \overbrace{[q_1 k_4 p_i + k_8 p_c q + p_1\gamma_2 p_i q]}^{k_9},$$

and $\eta_1 = 1-\eta$.

Since both coefficients of the first equation of (9) are positive, it follows that the real parts of the solution of (9) are negative. From the second equation of (9), we have that

$s_1 = -\frac{k_6\eta}{[(1-\eta)k_6+1]}$ is one solution, and the other solutions are the root of $\mathcal{T}(s) := A_5s^4 + A_1s^3 + A_2s^2 + A_3s + A_4$. Note that $A_4 > 0 \Longleftrightarrow \mathcal{R}_c < 1$, and $\mathcal{R}_c < 1 \Longrightarrow (A_1 > 0, A_2 > 0, A_3 > 0, \text{ and } A_5 > 0)$. Then, it follows that, if $\mathcal{R}_c < 1$, then the disease-free equilibrium $\mathcal{Q}_0$ is asymptotically stable whenever the following Routh–Hurwitz criteria $\frac{A_1A_2}{A_5^2} - \frac{A_3}{A_5} > 0$ and $\frac{A_1A_2A_3}{A_5^3} - \frac{A_1^2A_4}{A_5^3} - \frac{A_3^2}{A_5^2} > 0$ are satisfied for polynomial $\mathcal{T}(s)$.

For uniform stability, we use the Lyapunov function:

$$\mathcal{M}(E, C, I, B) = \mathbf{b}_1E(t) + \mathbf{b}_2C(t) + \mathbf{b}_3I(t) + \mathbf{b}_4B(t), \tag{10}$$

where $\mathbf{b}_1 = 1$, $\mathbf{b}_2 = k_3(k_8p_c + p_ip_1\gamma_2)/[k_4p_iq_1\gamma_1 + q\gamma_1(k_8p_c + p_ip_1\gamma_2)]$, and $\mathbf{b}_3 = k_3k_4p_i/[k_4p_iq_1\gamma_1 + q\gamma_1(k_8p_c + p_ip_1\gamma_2)]$ and $\mathbf{b}_4 = k_3k_4k_8/[k_4p_iq_1\gamma_1 + q\gamma_1(k_8p_c + p_ip_1\gamma_2)]$.

The fractional derivative of $\mathcal{M}$ is given by

$$\begin{aligned}
{}_{t_0}^{C}D_t^{\eta}\mathcal{M}(E, C, I, B) \leq\ & {}_{t_0}^{C}D_t^{\eta}E\mathbf{b}_1 + {}_{t_0}^{C}D_t^{\eta}C\mathbf{b}_2 + {}_{t_0}^{C}D_t^{\eta}I\mathbf{b}_3 + {}_{t_0}^{C}D_t^{\eta}B\mathbf{b}_4 \\
&= \mathbf{b}_1(\nu B[S + \pi V] - k_3E) + \mathbf{b}_2(q\gamma_1E - k_4C) + \mathbf{b}_3(q_1\gamma_1E + p_1\gamma_2C - k_8I) \\
&+ \mathbf{b}_4(p_cC + p_iI - \mu_bB) \\
&\leq \mathbf{b}_1\left(\nu B\left[S^0 + \pi V^0\right] - k_3E\right) + \mathbf{b}_2(q\gamma_1E - k_4C) + \mathbf{b}_3(q_1\gamma_1E + p_1\gamma_2C - k_8I) \\
&+ \mathbf{b}_4(p_cC + p_iI - \mu_bB) \\
&= \mathbf{b}_1\nu B\left(S^0 + \pi V^0\right) - \mathbf{b}_1k_3E + \mathbf{b}_2q\gamma_1E - \mathbf{b}_2k_4C + \mathbf{b}_3q_1\gamma_1E + \mathbf{b}_3p_1\gamma_2C \\
&- \mathbf{b}_3k_8I + \mathbf{b}_4p_cC + \mathbf{b}_4p_iI - \mathbf{b}_4\mu_bB \\
&= \mathbf{b}_1\nu B\left(S^0 + \pi V^0\right) - \mathbf{b}_4\mu_bB + (\mathbf{b}_3q_1\gamma_1 + \mathbf{b}_2q\gamma_1 - \mathbf{b}_1k_3)E \\
&+ (\mathbf{b}_4p_c + \mathbf{b}_3p_1\gamma_2 - \mathbf{b}_2k_4)C + (\mathbf{b}_4p_i - \mathbf{b}_3k_8)I \\
&= \frac{\mu_bk_3k_4(k_5 + \sigma)}{p_iq_1\gamma_1k_4 + q\gamma_1(p_1p_i\gamma_2 + p_c(k_5 + \sigma))}\left(\mathcal{R}_c^2 - 1\right)B.
\end{aligned}$$

Thus, ${}_{t_0}^{C}D_t^{\eta}\mathcal{M}(E, C, I, B) < 0$ whenever $\mathcal{R}_c < 1$, and ${}_{t_0}^{C}D_t^{\eta}\mathcal{M}(E, C, I, B) = 0$ if and only if $\mathcal{R}_c = 1$ or $B(\zeta) = 0$. Setting $B = 0$ in (5), we obtain $S = S_0$, $V = V_0$, and $E = C = I = R = 0$. Thus, $\lim_{t\to\infty}(S(t), V(t), E(t), C(t), I(t), R(t))' \to (S_0, V_0, 0, 0, 0, 0, 0)' := \mathcal{Q}_0$. Consequently, by [31] (Theorem 2.5), it follows that if $\mathcal{R}_c < 1$, then $\mathcal{Q}_0$ is uniformly asymptotically stable in $\mathcal{W}$. □

Existence and Uniqueness Analysis

Before describing the existence and uniqueness of solutions for the fractional model using the fixed point theorem, we define $\mathcal{T}$ as a Banach space of continuous functions defined on an interval $\mathcal{P}$ with the norm

$$\| \mathbf{X} \| = \sum_{i=1}^{i=7} \| \mathbf{X}_i \|,$$

where $\mathbf{X} = (S, V, E, C, I, R, B)$, $\| \mathbf{X}_i \| = \sup\{|\mathbf{X}_i(t)| : t \in \mathcal{P}\}$, and $\mathcal{T} = \mathcal{M}(\mathcal{P}) \times \mathcal{M}(\mathcal{P}) \times \mathcal{M}(\mathcal{P}) \times \mathcal{M}(\mathcal{P}) \times \mathcal{M}(\mathcal{P}) \times \mathcal{M}(\mathcal{P}) \times \mathcal{M}(\mathcal{P})$.

Let us write system (5) as follows:

$$\begin{aligned}
{}^{C}D_t^{\eta} S(t) &= \mathbf{H}_1(t, S),\\
{}^{C}D_t^{\eta} V(t) &= \mathbf{H}_2(t, V),\\
{}^{C}D_t^{\eta} E(t) &= \mathbf{H}_3(t, E),\\
{}^{C}D_t^{\eta} C(t) &= \mathbf{H}_4(t, C)\\
{}^{C}D_t^{\eta} I(t) &= \mathbf{H}_5(t, I)\\
{}^{C}D_t^{\eta} R(t) &= \mathbf{H}_6(t, R)\\
{}^{C}D_t^{\eta} B(t) &= \mathbf{H}_7(t, B)
\end{aligned} \tag{11}$$

Application of the Caputo fractional integral operator permits us to reduce (11) to the following system:

$$\begin{aligned}
-S(0) + S(t) &= \left[\int_0^t (t-\varsigma)^{\eta-1}\mathbf{H}_1(\varsigma, S)d\varsigma\right]\frac{1}{\Gamma(\eta)},\\
-V(0) + V(t) &= \left[\int_0^t (t-\varsigma)^{\eta-1}\mathbf{H}_2(\varsigma, V)d\varsigma\right]\frac{1}{\Gamma(\eta)},\\
-E(0) + E(t) &= \left[\int_0^t (t-\varsigma)^{\eta-1}\mathbf{H}_3(\varsigma, E)d\varsigma\right]\frac{1}{\Gamma(\eta)},\\
-C(0) + C(t) &= \left[\int_0^t (t-\varsigma)^{\eta-1}\mathbf{H}_4(\varsigma, C)d\varsigma\right]\frac{1}{\Gamma(\eta)},\\
-I(0) + I(t) &= \left[\int_0^t (t-\varsigma)^{\eta-1}\mathbf{H}_5(\varsigma, I)d\varsigma\right]\frac{1}{\Gamma(\eta)},\\
-R(0) + R(t) &= \left[\int_0^t (t-\varsigma)^{\eta-1}\mathbf{H}_6(\varsigma, R)d\varsigma\right]\frac{1}{\Gamma(\eta)},\\
-B(0) + B(t) &= \left[\int_0^t (t-\varsigma)^{\eta-1}\mathbf{H}_7(\varsigma, R)d\varsigma\right]\frac{1}{\Gamma(\eta)},
\end{aligned} \tag{12}$$

with $0 < \eta < 1$.

Now, we will provide the Lipschitz conditions fulfilled by $\mathbf{H}_i$, for $i = 1, 2, \ldots, 7$, as well as the contraction conditions. In the following theorem, we only provide the condition for $\mathbf{H}_1$, the rest being similar.

Theorem 3. *The kernel* $\mathbf{H}_1$ *satisfies the Lipschitz and contraction conditions provided that* $0 \leq \nu\kappa_7 + k_1 < 1$.

Proof. For S, we proceed as below:

$$\begin{aligned}
\| \mathbf{H}_1(t, S) - \mathbf{H}_1(t, S_1) \| &= \| -\nu B(S - S_1) - k_1(S - S_1) \|\\
&= \| \nu B + k_1 \| \| (S(t) - S_1(t)) \|\\
&\leq \| \nu\kappa_7 + k_1 \| \| S(t) - S_1(t) \|
\end{aligned}$$

where κ_7 is the upper bound of the function $B(t)$. Now, setting $W_1 = \nu\kappa_7 + k_1$, we finally obtain

$$\| \mathbf{H}_1(t, S) - \mathbf{H}_1(t, S_1) \| \leq W_1 \| S(t) - S(t_1) \|, \tag{13}$$

which provide the Lipschitz condition. If, additionally, we can have $0 < W_1 = \nu\kappa_7 + k_1 < 1$, then the contraction is also obtained.

As in the case of $\mathbf{H}_1$, it is easy to obtain the Lipschitz condition for the other kernels. Thus, we have

$$\begin{aligned}
\| \mathbf{H}_2(t, C) - \mathbf{H}_2(t, C_1) \| &\leq W_2 \| V(t) - V(t_1) \|, \\
\| \mathbf{H}_3(t, E) - \mathbf{H}_3(t, E_1) \| &\leq W_3 \| E(t) - E(t_1) \|, \\
\| \mathbf{H}_4(t, C) - \mathbf{H}_4(t, C_1) \| &\leq W_4 \| C(t) - C(t_1) \|, \\
\| \mathbf{H}_5(t, I) - \mathbf{H}_5(t, I_1) \| &\leq W_5 \| I(t) - I(t_1) \|, \\
\| \mathbf{H}_6(t, R) - \mathbf{H}_6(t, R_1) \| &\leq W_6 \| R(t) - R(t_1) \|, \\
\| \mathbf{H}_7(t, B) - \mathbf{H}_7(t, B_1) \| &\leq W_7 \| B(t) - B(t_1) \| .
\end{aligned} \tag{14}$$

□

Recursively, Equation (12) can be rewritten as follows:

$$\begin{aligned}
S_n(t) - S(0) &= \frac{1}{\Gamma(\eta)} \int_0^t (t-\varsigma)^{\eta-1} \mathbf{H}_1(\varsigma, S_{n-1}) d\varsigma, \\
V_n(t) - V(0) &= \frac{1}{\Gamma(\eta)} \int_0^t (t-\varsigma)^{\eta-1} \mathbf{H}_2(\varsigma, V_{n-1}) d\varsigma, \\
E_n(t) - E(0) &= \frac{1}{\Gamma(\eta)} \int_0^t (t-\varsigma)^{\eta-1} \mathbf{H}_3(\varsigma, E_{n-1}) d\varsigma, \\
C_n(t) - C(0) &= \frac{1}{\Gamma(\eta)} \int_0^t (t-\varsigma)^{\eta-1} \mathbf{H}_4(\varsigma, C_{n-1}) d\varsigma, \\
I_n(t) - I(0) &= \frac{1}{\Gamma(\eta)} \int_0^t (t-\varsigma)^{\eta-1} \mathbf{H}_5(\varsigma, I_{n-1}) d\varsigma, \\
R_n(t) - R(0) &= \frac{1}{\Gamma(\eta)} \int_0^t (t-\varsigma)^{\eta-1} \mathbf{H}_6(\varsigma, R_{n-1}) d\varsigma, \\
B_n(t) - B(0) &= \frac{1}{\Gamma(\eta)} \int_0^t (t-\varsigma)^{\eta-1} \mathbf{H}_7(\varsigma, B_{n-1}) d\varsigma.
\end{aligned} \tag{15}$$

By determing, in a recursive manner, the difference between the successive terms of (11), we obtain

$$\begin{aligned}
\psi_{1n}(t) = S_n(t) - S_{n-1}(t) &= \frac{1}{\Gamma(\eta)} \int_0^t (t-\varsigma)^{\eta-1} (\mathbf{H}_1(\varsigma, S_{n-1}) - \mathbf{H}_1(\varsigma, S_{n-2})) d\varsigma, \\
\psi_{2n}(t) = V_n(t) - V_{n-1}(t) &= \frac{1}{\Gamma(\eta)} \int_0^t (t-\varsigma)^{\eta-1} (\mathbf{H}_2(\varsigma, V_{n-1}) - \mathbf{H}_2(\varsigma, V_{n-2})) d\varsigma, \\
\psi_{3n}(t) = E_n(t) - E_{n-1}(t) &= \frac{1}{\Gamma(\eta)} \int_0^t (t-\varsigma)^{\eta-1} (\mathbf{H}_3(\varsigma, E_{n-1}) - \mathbf{H}_3(\varsigma, E_{n-2})) d\varsigma, \\
\psi_{4n}(t) = C_n(t) - C_{n-1}(t) &= \frac{1}{\Gamma(\eta)} \int_0^t (t-\varsigma)^{\eta-1} (\mathbf{H}_4(\varsigma, C_{n-1}) - \mathbf{H}_4(\varsigma, C_{n-2})) d\varsigma, \\
\psi_{5n}(t) = I_n(t) - I_{n-1}(t) &= \frac{1}{\Gamma(\eta)} \int_0^t (t-\varsigma)^{\eta-1} (\mathbf{H}_5(\varsigma, I_{n-1}) - \mathbf{H}_5(\varsigma, I_{n-2})) d\varsigma, \\
\psi_{6n}(t) = R_n(t) - R_{n-1}(t) &= \frac{1}{\Gamma(\eta)} \int_0^t (t-\varsigma)^{\eta-1} (\mathbf{H}_6(\varsigma, R_{n-1}) - \mathbf{H}_6(\varsigma, R_{n-2})) d\varsigma, \\
\psi_{7n}(t) = B_n(t) - B_{n-1}(t) &= \frac{1}{\Gamma(\eta)} \int_0^t (t-\varsigma)^{\eta-1} (\mathbf{H}_7(\varsigma, B_{n-1}) - \mathbf{H}_7(\varsigma, B_{n-2})) d\varsigma,
\end{aligned} \tag{16}$$

with $S_0(t) = S(0)$, $V_0(t) = V(0)$, $E_0(t) = E(0)$, $C_0(t) = C(0)$, $I_0(t) = I(0)$, $R_0(t) = R(0)$, and $B_0(t) = B(0)$.

The norm of $\phi_{1n}(t)$ gives

$$\begin{aligned} \| \psi_{1n}(t) \| = \| S_n(t) - S_{n-1}(t) \| &= \| \frac{1}{\Gamma(\eta)} \int_0^t (t-\varsigma)^{\eta-1} (\mathbf{H}_1(\varsigma, S_{n-1}) - \mathbf{H}_1(\varsigma, S_{n-2})) d\varsigma \| \\ &\leq \frac{1}{\Gamma(\eta)} \| \int_0^t (t-\varsigma)^{\eta-1} (\mathbf{H}_1(\varsigma, S_{n-1}) - \mathbf{H}_1(\varsigma, S_{n-2})) d\varsigma \| . \end{aligned} \tag{17}$$

With the Lipschitz condition (13), we obtain

$$\| \psi_{1n}(t) \| = \| S_n(t) - S_{n-1}(t) \| \leq \frac{1}{\Gamma(\eta)} W_1 \int_0^t (t-\varsigma)^{\eta-1} \| S_{n-1} - S_{n-2} \| d\varsigma. \tag{18}$$

Thus, we have

$$\| \psi_{1n}(t) \| \leq \frac{1}{\Gamma(\eta)} W_1 \int_0^t (t-\varsigma)^{\eta-1} \| \psi_{1(n-1)}(\varsigma) \| d\varsigma. \tag{19}$$

By proceeding in a similar way, we obtain, for the other $\phi_{in}(t)$, $i = 2, \ldots, 7$,

$$\begin{aligned} \| \psi_{2n}(t) \| &\leq \frac{1}{\Gamma(\eta)} W_2 \int_0^t (t-\varsigma)^{\eta-1} \| \psi_{2(n-1)}(\varsigma) \| d\varsigma, \\ \| \psi_{3n}(t) \| &\leq \frac{1}{\Gamma(\eta)} W_3 \int_0^t (t-\varsigma)^{\eta-1} \| \psi_{3(n-1)}(\varsigma) \| d\varsigma, \\ \| \psi_{4n}(t) \| &\leq \frac{1}{\Gamma(\eta)} W_4 \int_0^t (t-\varsigma)^{\eta-1} \| \psi_{4(n-1)}(\varsigma) \| d\varsigma, \\ \| \psi_{5n}(t) \| &\leq \frac{1}{\Gamma(\eta)} W_5 \int_0^t (t-\varsigma)^{\eta-1} \| \psi_{5(n-1)}(\varsigma) \| d\varsigma, \\ \| \psi_{6n}(t) \| &\leq \frac{1}{\Gamma(\eta)} W_6 \int_0^t (t-\varsigma)^{\eta-1} \| \psi_{6(n-1)}(\varsigma) \| d\varsigma, \\ \| \psi_{7n}(t) \| &\leq \frac{1}{\Gamma(\eta)} W_7 \int_0^t (t-\varsigma)^{\eta-1} \| \psi_{7(n-1)}(\varsigma) \| d\varsigma. \end{aligned} \tag{20}$$

Each nth term of the state variables of (5) is given by

$$\begin{cases} S_n(t) = \sum\limits_{i=1}^{n} \psi_{1i}(t), V_n(t) = \sum\limits_{i=1}^{n} \psi_{2i}(t), E_n(t) = \sum\limits_{i=1}^{n} \psi_{3i}(t), \\ C_n(t) = \sum\limits_{i=1}^{n} \psi_{4i}(t), I_n(t) = \sum\limits_{i=1}^{n} \psi_{5i}(t), R_n(t) = \sum\limits_{i=1}^{n} \psi_{6i}(t), \\ B_n(t) = \sum\limits_{i=1}^{n} \psi_{7i}(t). \end{cases} \tag{21}$$

The following result guarantees that the solution of the fractional model (5) is unique.

Theorem 4. *If the following inequality holds,*

$$\frac{1}{\Gamma(\eta)} \mathbf{x}^{\eta} W_i < 1, \quad \text{for} \quad i = 1, 2, \ldots, 7, \tag{22}$$

then the solution of the fractional model (5)*, for* $t \in [0, T]$*, is unique.*

Proof. With Equation (13), inequalities (19) and (20), combined with a recursive technique, we obtain:

$$\begin{aligned}
&\| \psi_{1n}(t) \| \leq \| S_0(t) \| \left[\frac{W_1}{\Gamma(\eta)}\mathbf{x}^{\eta}\right]^n, \| \psi_{2n}(t) \| \leq \| W_0(t) \| \left[\frac{W_2}{\Gamma(\eta)}\mathbf{x}^{\eta}\right]^n,\\
&\| \psi_{3n}(t) \| \leq \| E_0(t) \| \left[\frac{W_3}{\Gamma(\eta)}\mathbf{x}^{\eta}\right]^n, \| \psi_{4n}(t) \| \leq \| C_0(t) \| \left[\frac{W_4}{\Gamma(\eta)}\mathbf{x}^{\eta}\right]^n,\\
&\| \psi_{5n}(t) \| \leq \| I_0(t) \| \left[\frac{W_5}{\Gamma(\eta)}\mathbf{x}^{\eta}\right]^n, \| \psi_{6n}(t) \| \leq \| R_0(t) \| \left[\frac{W_6}{\Gamma(\eta)}\mathbf{x}^{\eta}\right]^n,\\
&\| \psi_{7n}(t) \| \leq \| B_0(t) \| \left[\frac{W_7}{\Gamma(\eta)}\mathbf{x}^{\eta}\right]^n.
\end{aligned} \tag{23}$$

Therefore, the above sequences satisfy $\lim_{n\to\infty} \| \psi_{in}(t) \| \to 0$, $j = 1, 2, \ldots, 7$. The triangle inequality applied to (23) permits us to obtain

$$\begin{aligned}
\| S_{k+n}(t) - S_n(t) \| &\leq \sum_{j=n+1}^{k+n} \mathbf{Z}_1^j = \frac{\mathbf{Z}_1^{n+1} - \mathbf{Z}_1^{k+n+1}}{1-\mathbf{Z}_1},\\
\| V_{k+n}(t) - V_n(t) \| &\leq \sum_{j=n+1}^{k+n} \mathbf{Z}_2^j = \frac{\mathbf{Z}_2^{n+1} - \mathbf{Z}_2^{k+n+1}}{1-\mathbf{Z}_2},\\
\| E_{k+n}(t) - E_n(t) \| &\leq \sum_{j=n+1}^{k+n} \mathbf{Z}_3^j = \frac{\mathbf{Z}_3^{n+1} - \mathbf{Z}_3^{k+n+1}}{1-\mathbf{Z}_3},\\
\| C_{k+n}(t) - C_n(t) \| &\leq \sum_{j=n+1}^{k+n} \mathbf{Z}_4^j = \frac{\mathbf{Z}_4^{n+1} - \mathbf{Z}_4^{k+n+1}}{1-\mathbf{Z}_4},\\
\| I_{k+n}(t) - I_n(t) \| &\leq \sum_{j=n+1}^{k+n} \mathbf{Z}_5^j = \frac{\mathbf{Z}_5^{n+1} - \mathbf{Z}_5^{k+n+1}}{1-\mathbf{Z}_5},\\
\| R_{k+n}(t) - R_n(t) \| &\leq \sum_{j=n+1}^{k+n} \mathbf{Z}_6^j = \frac{\mathbf{Z}_6^{n+1} - \mathbf{Z}_6^{k+n+1}}{1-\mathbf{Z}_6},\\
\| B_{k+n}(t) - B_n(t) \| &\leq \sum_{j=n+1}^{k+n} \mathbf{Z}_7^j = \frac{\mathbf{Z}_7^{n+1} - \mathbf{Z}_7^{n+k+1}}{1-\mathbf{Z}_7},
\end{aligned} \tag{24}$$

with $\frac{1}{\Gamma(\eta)} b^{\eta} W_l < 1$ and $\mathbf{Z}_l = \left(\frac{1}{\Gamma(\eta)} W_l \mathbf{x}^{\eta}\right)^n$, $l = 1, 2, \ldots, 7$.

Therefore, S_n, V_n, E_n, C_n, I_n, R_n, and B_n are uniformly convergent Cauchy sequences (see [32]). With $n \to \infty$, it follows that the limit of these sequences represents the unique solution to model (5). □

Numerical Scheme of the Fractional Model and Its Stability Analysis

Several methods have been developed to construct numerical schemes for fractional models. One can cite, among others, the Implicit Quadrature method [24], the Approximate Mittag–Leffler method [33], the Predictor Corrector method [34], and the Adams–Bashforth–Moulton method [25]. The choice of the method depends on several factors, such as the amount of information treated [35] and the accuracy order [36]. The numerical scheme proposed in this work is constructed using the Adams–Bashforth–Moulton method.

Let us consider the following general form of a fractional differential equation [37]:

$$\begin{cases} \mathbb{D}_t^{\eta} \varphi(t) &= h(t, \varphi(t)), \quad 0 \leq t \leq T,\\ \varphi^{(l)}(0) &= \varphi_0^l, \qquad\quad l = 0, 1, 2, \ldots, n-1, \textit{where } n = [\eta], \end{cases} \tag{25}$$

which is equivalent to

$$\varphi(t) = \sum_{l=0}^{n-1} h_0^l \frac{t^l}{l!} + \frac{1}{\Gamma(\eta)} \int_0^t (t-\zeta)^{\eta-1} h(\zeta, \varphi(\zeta)) d\zeta. \tag{26}$$

For $\eta \in [0,1]$, $0 \le t \le T$ and setting $\kappa = T/N$ and $t_m = m\kappa$, for $m = 0, 1, 2, \ldots, N \in \mathbb{Z}^+$, the solution of the fractional model is

$$\begin{aligned}
S_{1+m} &= S_0 + \frac{\kappa^\eta}{\Gamma(\eta+2)}\left(\Lambda_h + \eta R_{1+m}^p + \theta V_{1+m}^p - (\nu B_{1+m}^p + k_1) S_{1+m}^p\right) \\
&\quad + \frac{\kappa^\eta}{\Gamma(\eta+2)} \sum_{j=0}^{m} a_{j,1+m}\left(\Lambda_h + \eta R_j + \theta V_j - (\nu B_j + k_1) S_j\right), \\
V_{1+m} &= V_0 + \frac{\kappa^\eta}{\Gamma(\eta+2)}\left(\xi S_{1+m}^p - \left[(1-\epsilon)\nu B_{1+m}^p + k_2\right] V_{1+m}^p\right) \\
&\quad + \frac{\kappa^\eta}{\Gamma(\eta+2)} \sum_{j=0}^{m} a_{j,1+m}\left(\xi S_j - \left[(1-\epsilon)\nu B_j + k_2\right] V_j\right), \\
E_{1+m} &= E_0 + \frac{\kappa^\eta}{\Gamma(\eta+2)}\left(\nu B_{1+m}^p \left[S_{1+m}^p + \pi V_{1+m}^p\right] - k_3 E_{1+m}^p\right) \\
&\quad + \frac{\kappa^\eta}{\Gamma(\eta+2)} \sum_{j=0}^{m} a_{j,1+m}\left(\nu B_j \left[S_j + \pi V_j\right] - k_3 E_j\right), \\
C_{1+m} &= C_0 + \frac{\kappa^\eta}{\Gamma(\eta+2)}\left(q\gamma_1 E_{1+m}^p - k_4 C_{1+m}^p\right) + \frac{\kappa^\eta}{\Gamma(\eta+2)} \sum_{j=0}^{m} a_{j,1+m}\left(q\gamma_1 E_j - k_4 C_j\right), \\
I_{1+m} &= I_0 + \frac{\kappa^\eta}{\Gamma(\eta+2)}\left(q_1\gamma_1 E_{1+m}^p + p_1\gamma_2 C_{1+m}^p - [k_5+\sigma] I_{1+m}^p\right) \\
&\quad + \frac{\kappa^\eta}{\Gamma(\eta+2)} \sum_{j=0}^{m} a_{j,1+m}\left(q_1\gamma_1 E_j + p_1\gamma_2 C_j - [k_5+\sigma] I_j\right), \\
R_{1+m} &= R_0 + \frac{\kappa^\eta}{\Gamma(\eta+2)}\left(p\gamma_2 C_{1+m}^p + \sigma I_{1+m}^p - k_6 R_{1+m}^p\right) + \frac{\kappa^\eta}{\Gamma(\eta+2)} \sum_{j=0}^{m} a_{j,1+m}\left(p\gamma_2 C_j + \sigma I_j - k_6 R_j\right), \\
B_{1+m} &= B_0 + \frac{\kappa^\eta}{\Gamma(\eta+2)}\left(p_c C_{1+m}^p + p_i I_{1+m}^p - \mu_b B_{1+m}^p\right) + \frac{\kappa^\eta}{\Gamma(\eta+2)} \sum_{j=0}^{m} a_{j,1+m}\left(p_c C_j + p_i I_j - \mu_b B_j\right),
\end{aligned} \tag{27}$$

where

$$\begin{aligned}
S^p_{1+m} &= S_0 + \frac{1}{\Gamma(\eta)}\sum_{j=0}^{m} b_{j,1+m}\Big(\Lambda_h + \eta R_j + \theta V_j - (\nu B_j + k_1)S_j\Big),\\
V^p_{1+m} &= V_0 + \frac{1}{\Gamma(\eta)}\sum_{j=0}^{m} b_{j,1+m}\Big(\xi S_j - \big[(1-\epsilon)\nu B_j + k_2\big]V_j\Big),\\
E^p_{1+m} &= E_0 + \frac{1}{\Gamma(\eta)}\sum_{j=0}^{m} b_{j,1+m}\Big(\nu B_j\big[S_j + \pi V_j\big] - k_3 E_j\Big),\\
C^p_{1+m} &= C_0 + \frac{1}{\Gamma(\eta)}\sum_{j=0}^{m} b_{j,1+m}\Big(q\gamma_1 E_j - k_4 C_j\Big),\\
I^p_{1+m} &= I_0 + \frac{1}{\Gamma(\eta)}\sum_{j=0}^{m} b_{j,1+m}\Big(= q_1\gamma_1 E_j + p_1\gamma_2 C_j - [k_5+\sigma]I_j\Big),\\
R^p_{1+m} &= R_0 + \frac{1}{\Gamma(\eta)}\sum_{j=0}^{m} b_{j,1+m}\Big(p\gamma_2 C_j + \sigma I_j - k_6 R_j\Big),\\
B^p_{1+m} &= B_0 + \frac{1}{\Gamma(\eta)}\sum_{j=0}^{m} b_{j,1+m}\Big(p_c C_j + p_i I_j - \mu_b B_j\Big),
\end{aligned} \tag{28}$$

and

$$a_{j,1+m} = \begin{cases} m^{\eta+1} - (m+1)(-\eta+m), & j=0,\\ (2-j+m)^{\eta+1} - 2(m-j+1)^{1+\eta} + (-j+m)^{1+\eta} & 1\le j\le m,\\ 1, & j = 1+m, \end{cases}$$

$$b_{j,1+m} = \frac{\kappa^\eta}{\eta}\big((m+1-j)^\eta - (m-j)^\eta\big),\ 0\le j\le m.$$

We then claim the following result.

Theorem 5. *Under some conditions, the above numerical scheme (see Equations (27) and (28)) is stable.*

Proof. Let $S^\star_0$, $S^\star_j (j = 0,\dots,1+m)$ and $S^{\star p}_{1+m}(m = 0,\dots,N-1)$ be perturbations of S_0, S_j, and S^p_{1+m}, respectively. By using Equations (19) and (28), the following perturbation equations are obtained:

$$S^{\star p}_{1+m} = S^\star_0 + \frac{1}{\Gamma(\eta)}\sum_{j=0}^{m} b_{j,1+m}(\mathcal{G}_1(t_j, S_j + S^\star_j) - \mathcal{G}_1(t_j, S_j)), \tag{29}$$

$$\begin{aligned}
S^\star_{1+m} = S^\star_0 &+ \frac{\kappa^\eta}{\Gamma(\eta+2)}(\mathcal{G}_1(t_{1+m}, S^p_{1+m} + S^P_{1+m}) - \mathcal{G}_1(t_{1+m}, S^p_{1+m}))\\
&+ \frac{\kappa^\eta}{\Gamma(\eta+2)}\sum_{j=0}^{m} a_{j,1+m}(\mathcal{G}_1(t_j, S_j + S^\star_j) - \mathcal{G}_1(t_j, S_j)).
\end{aligned} \tag{30}$$

The Lipschitz condition permits us to obtain

$$|S^\star_{1+m}| \le \phi_0 + \frac{\kappa^\eta M}{\Gamma(\eta+2)}\Big(|S^{\star p}_{1+m}| + \sum_{j=1}^{m} a_{j,1+m}|S^\star_j|\Big), \tag{31}$$

where $\phi_0 = \max_{0\leq m\leq N}\left\{|S_0^\star| + \frac{\kappa^\eta M a_{m,0}}{\Gamma(\eta+2)}|S_0^\star|\right\}$. From [32] (Equation (3.18)), it follows that

$$|S_{1+m}^{\star p}| \leq \Theta_0 + \frac{M}{\Gamma(\eta)}\sum_{j=1}^{m} b_{j,1+m}|S_j^\star|, \tag{32}$$

where $\Theta_0 = \max_{0\leq m\leq N}\left\{|S_0^\star| + \frac{M b_{m,0}}{\Gamma(\eta)}|S_0^\star|\right\}$. Substituting $|S_{1+m}^{\star p}|$ from Equation (32) into Equation (31) gives

$$\begin{aligned}
|S_{1+m}^\star| &\leq \varrho_0 + \frac{\kappa^\eta M}{\Gamma(\eta+2)}\left(\frac{M}{\Gamma(\eta)}\sum_{j=1}^{m} b_{j,1+m}|S_j^\star| + \sum_{j=1}^{m} a_{j,1+m}|S_j^\star|\right)\\
&\leq \varrho_0 + \frac{\kappa^\eta M}{\Gamma(\eta+2)}\sum_{j=1}^{m}\left(\frac{M}{\Gamma(\eta)}b_{j,1+m} + a_{j,1+m}\right)|S_j^\star|\\
&\leq \varrho_0 + \frac{\kappa^\eta M \mathcal{C}_{\eta,2}}{\Gamma(\eta+2)}\sum_{j=1}^{m}(m+1-j)^{\eta-1}|S_j^\star|,
\end{aligned} \tag{33}$$

where $\varrho_0 = \max\{\phi_0 + \frac{\kappa^\eta M a_{1+m,1+m}}{\Gamma(\eta+2)}\Theta_0\}$.

Thanks to Lemma 2, we have that $\mathcal{C}_{\eta,2} > 0$ and depends only on η, and κ is assumed to be small enough. A direct application of Lemma 1 implies $|S_{1+m}^\star| \leq \mathcal{C}\varrho_0$. The proof for the other variables is obtained in the same way. This ends the proof. □

2.3. Model Dynamics with the Standard Incidence Law

In this section, we extend model (2) by replacing the mass action incidence law with the standard incidence law, and considering direct transmission (human to human). The new typhoid fever transmission dynamics model is thus presented as follows:

$$\dot{S}(t) = \Lambda_h + \theta V(t) + \alpha R(t) - k_1 S(t) - \beta\frac{(I+C)}{N(t)}S(t) - \nu\frac{B(t)}{B(t)+K}S(t), \tag{34a}$$

$$\dot{V}(t) = -\left[k_2 + \pi\beta\frac{(C+I)}{N(t)} + \pi\nu\frac{B(t)}{K+B(t)}\right]V(t) + \xi S(t), \tag{34b}$$

$$\dot{E}(t) = \left[\beta\frac{(C+I)}{N(t)} + \nu\frac{B(t)}{B(t)+K}\right](\pi V(t) + S(t)) - k_3 E(t), \tag{34c}$$

$$\dot{C}(t) = q\gamma_1 E(t) - k_4 C(t), \tag{34d}$$

$$\dot{I}(t) = q_1\gamma_1 E(t) + p_1\gamma_2 C(t) - k_8 I(t), \tag{34e}$$

$$\dot{R}(t) = p\gamma_2 C(t) + \sigma I(t) - k_6 R(t), \tag{34f}$$

$$\dot{B}(t) = p_c C(t) + p_i I(t) - \mu_b B(t), \tag{34g}$$

where β is the direct transmission rate, and K represents the half-saturation constant.

The corresponding fractional model is given by

$$
\begin{aligned}
{}_{t_0}^{C}D_t^{\eta} S(t) &= \Lambda_h + \theta V(t) + \alpha R(t) - k_1 S(t) - \beta \frac{(I+C)}{N(t)} S(t) - \nu \frac{B(t)}{K+B(t)} S(t), && \text{(35a)}\\
{}_{t_0}^{C}D_t^{\eta} V(t) &= -\left[k_2 + \pi\beta \frac{(I+C)}{N(t)} + \pi\nu \frac{B(t)}{K+B(t)}\right] V(t) + \xi S(t), && \text{(35b)}\\
{}_{t_0}^{C}D_t^{\eta} E(t) &= \left[\beta \frac{(I+C)}{N(t)} + \nu \frac{B(t)}{K+B(t)}\right] (\pi V(t) + S(t)) - k_3 E(t), && \text{(35c)}\\
{}_{t_0}^{C}D_t^{\eta} C(t) &= q\gamma_1 E(t) - k_4 C(t), && \text{(35d)}\\
{}_{t_0}^{C}D_t^{\eta} I(t) &= q_1\gamma_1 E(t) + p_1\gamma_2 C(t) - k_8 I(t), && \text{(35e)}\\
{}_{t_0}^{C}D_t^{\eta} R(t) &= p\gamma_2 C(t) + \sigma I(t) - k_6 R(t), && \text{(35f)}\\
{}_{t_0}^{C}D_t^{\eta} B(t) &= p_c C(t) + p_i I(t) - \mu_b B(t). && \text{(35g)}
\end{aligned}
$$

Without loss of generality, it is evident that the new model (34) (resp. (35)) is also defined in $\mathcal{W}$.

Model (34) has the same disease-free equilibrium as model system (2). Using the same approach developed in [29], we define the next-generation matrix of model system (34) as

$$
NGM = \begin{pmatrix}
R_1 & \frac{H_0 p_1 \gamma_2 \beta}{N_0 k_4 k_8} + \frac{H_0 \beta}{N_0 k_4} & \frac{H_0 \beta}{N_0 k_8} & R_4 \\
0 & 0 & 0 & 0 \\
0 & 0 & 0 & 0 \\
R_5 & \frac{p_1 \gamma_2 p_i}{k_4 k_8} + \frac{p_c}{k_4} & \frac{p_i}{k_8} & 0
\end{pmatrix}
$$

where $R_1 = \dfrac{H_0 \beta \gamma_1}{N_0 k_3 k_4}\left[\dfrac{(p_1\gamma_2 q + q_1 k_4)}{k_8} + q\right]$, $R_4 = \dfrac{H_0 \nu}{K\mu_b}$, $R_5 = \dfrac{\gamma_1}{k_3 k_4}\left[\dfrac{p_i(p_1\gamma_2 q + q_1 k_4)}{k_8} + p_c q\right]$, and $H_0 = S_0 + \pi V_0$.

Thus, the control reproduction number of model (34), which is the spectral radius of NGM, is given by

$$
\mathcal{R}_{c\star} = \frac{R_1 + \sqrt{R_1^2 + 4R_4 R_5}}{2}. \tag{36}
$$

The following result is a direct consequence of Theorem 2 in [29] (see Appendix A for the proof).

Proposition 3. *For model (34) (resp. (35)), $\mathcal{Q}_0$ is locally asymptotically stable in $\mathcal{W}$ if $\mathcal{R}_{c\star} < 1$ and unstable if $\mathcal{R}_{c\star} > 1$.*

Theorem 6. *For the new typhoid model (34) (resp. (35)), the disease-free equilibrium $\mathcal{Q}_0$ is globally asymptotically stable if $\mathcal{R}_{c\star} < 1$ and unstable otherwise.*

Proof. See Appendix B. □

3. Results

3.1. Numerical Results of the Fractional Model with Mass Action Incidence Law

We perform several simulations with the parameter values listed in Table 1.

Table 1. Parameter values of (2) taken from [5].

Parameter	Value	Parameter	Value	Parameter	Value
Λ_h	1	μ_b	0.149990	ν	3.2618×10^{-6}
γ_1	0.2145	ϵ	0.9495	δ	0.1499
γ_2	0.1498	ξ	0.3221	σ	0.49992
α	0.0834	θ	0.0833	$\mathcal{R}_c$	2.4750

The step size is $\kappa = 10^{-8}$, the initial time is $T = 0$, and the final time is $T > 0$. We begin by showing the impact of fractional order on the dynamics of the disease. To this aim, the fractional-order parameter varies between $\eta = 1$ and $\eta = 0.5$.

Figure 1 displays the impact of the Caputo fractional operator on the model dynamics. For different values of the fractional-order parameter η, the infected state profiles are drawn. From Figure 1, it follows that when the fractional order η decreases, the solutions of our fractional model (5) have different behaviors. Indeed, when the fractional order decreases, the number of infected humans in latent, carrier, and symptomatic states increases. This is the same for the compartment B. This phenomenon was also observed in a malaria fractional model studied by [38]. It is important to note that for $\eta = 1$, the solutions of the fractional model converge to the solutions of the integer model.

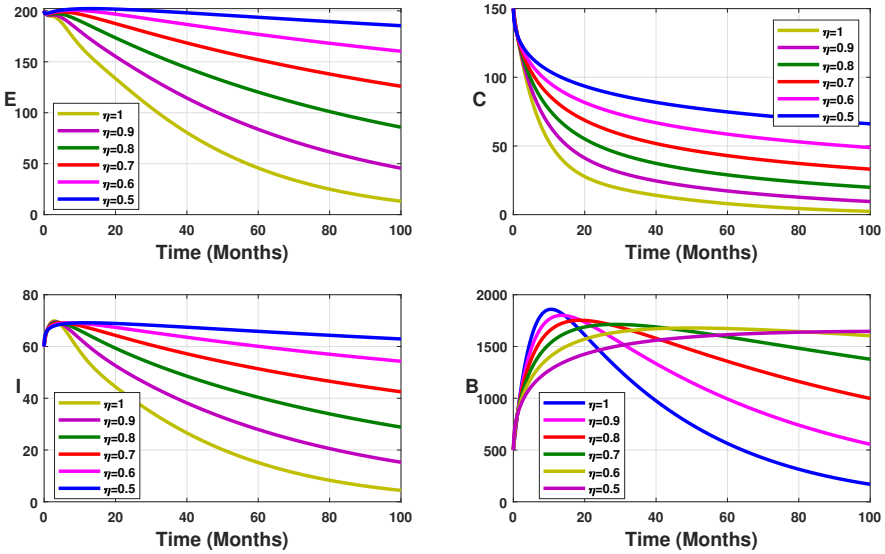

Figure 1. Simulation results showing the fractional dynamics on the infected state variable profiles for different values of the fractional-order parameter η.

To evaluate the impact of vaccination on typhoid fever transmission dynamics, we fix the vaccine efficacy at $\epsilon = 70\%$ while the vaccine coverage parameter varies between $\xi = 0\%$ and $\xi = 90\%$ ($\xi \in \{0.90, 0.50, 0.20, 0\}$), with different values of the fractional-order η ($\eta \in \{1, 0.90, 0.80, 0.70, 0.60, 0.50\}$). The results are displayed in Figures 2–5.

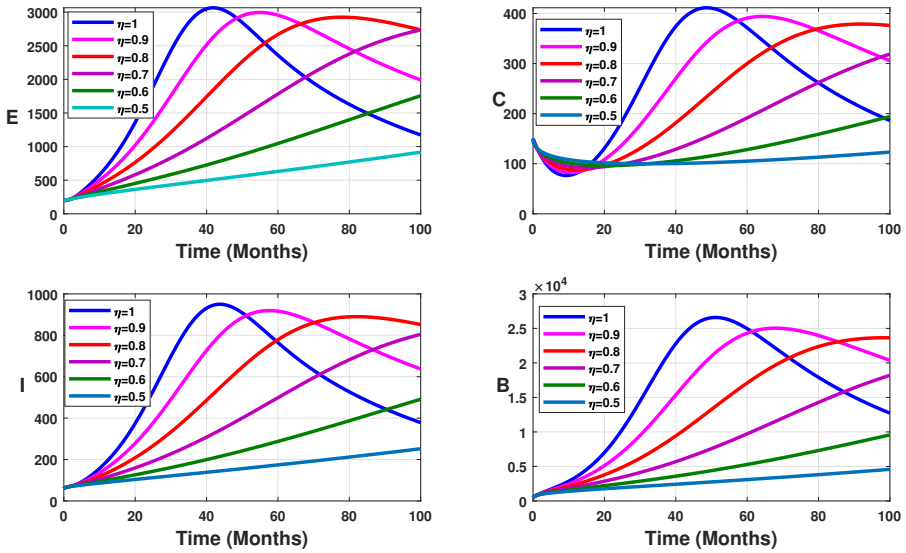

Figure 2. Simulation results showing the infected state variable profiles without vaccination ($\xi = 0$).

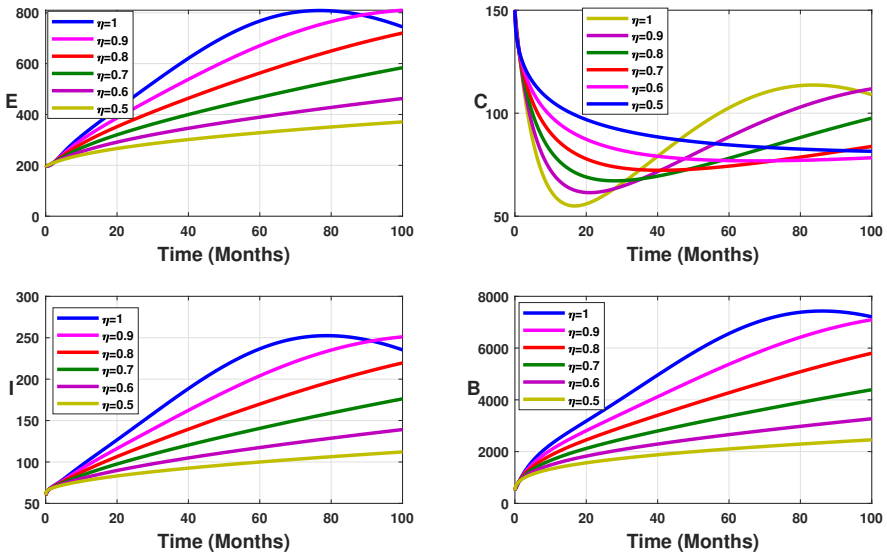

Figure 3. Simulation results showing the infected state variable profiles when the vaccination coverage $\xi = 20\%$ with different values of the fractional order.

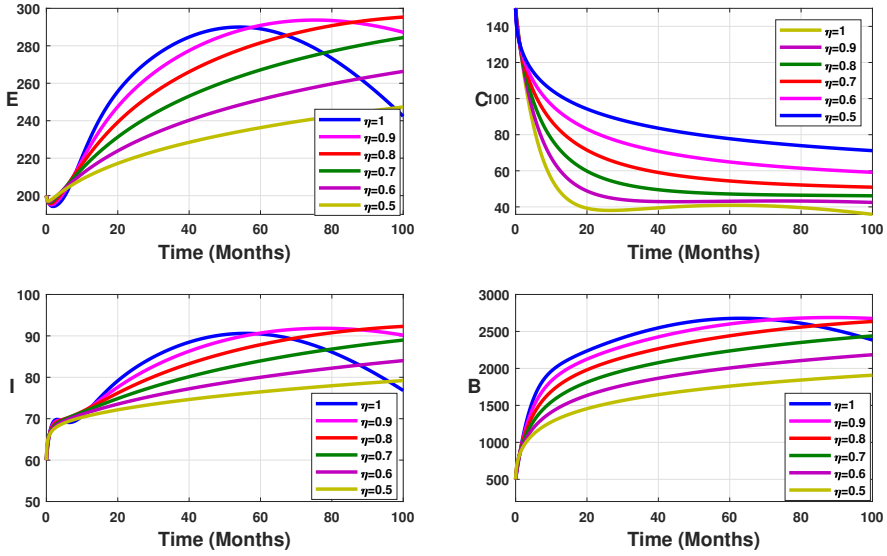

Figure 4. Simulation results showing the infected state variable profiles when the vaccination coverage $\xi = 50\%$ with different values of the fractional order.

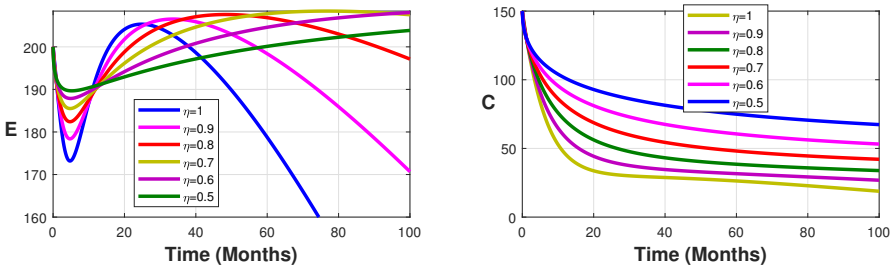

Figure 5. *Cont.*

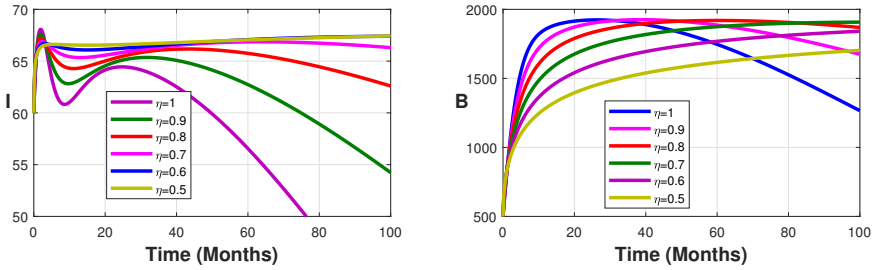

Figure 5. Simulation results showing the infected state variable profiles when the vaccination coverage $\xi = 90\%$ with different values of the fractional order.

Without vaccination coverage $\xi = 0$ (Figure 2), the peak delayed phenomenon is observable. Indeed, for $\eta = 1$, the peak date corresponds to $T = 45$ months, with approximately 3000 infected individuals in the latent stage, 400 asymptomatic individuals, 950 symptomatic individuals, and 26,000 free salmonella in the environment. This peak date is delayed when the fractional-order parameter η decreases. Thus, the peak dates are beyond $T = 45$ months. From Figures 3–5, we note that this peak date is forward delayed beyond $T = 45$ months whenever the fractional-order parameter η decreases. Moreover, the number of infected individuals decreases with the decrease in the fractional-order parameter.

Now, in addition to vaccination, we consider environmental sanitation. To this aim, the bacterial decay rate μ_b is modified to $\mu_b := \mu_b + \omega$, where $\omega \in \{0, 0.1, 0.2.0.3, 0.4\}$ represents the additional decay rate of free salmonella due to environmental sanitation [6]. The vaccination coverage is fixed at $\xi = 32.21\%$ as reported in Table 1. From Figures 6–9, it is evident that mass vaccination combined with environmental sanitation has a positive impact, reducing the disease burden.

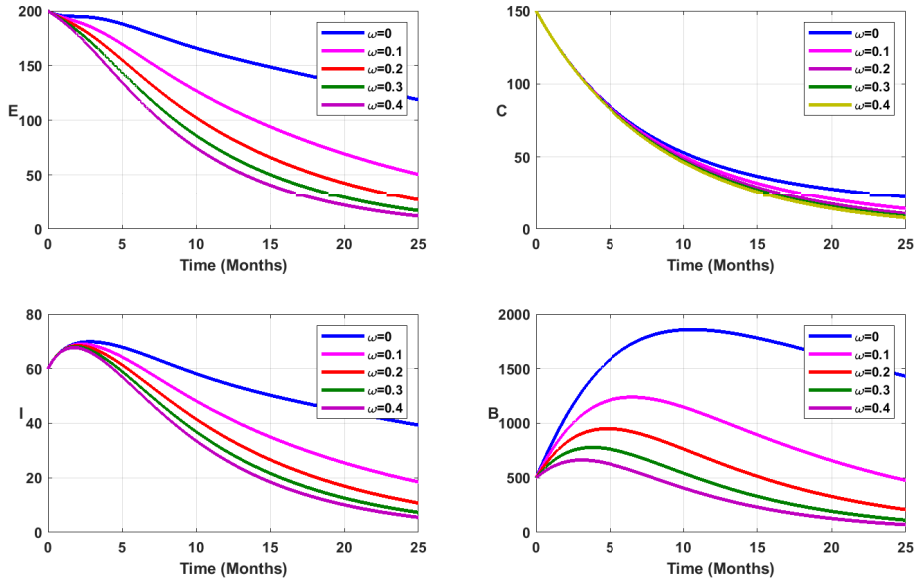

Figure 6. Simulation results showing the infected state variable profiles when vaccination is combined with environmental sanitation, for fractional order $\eta = 1$.

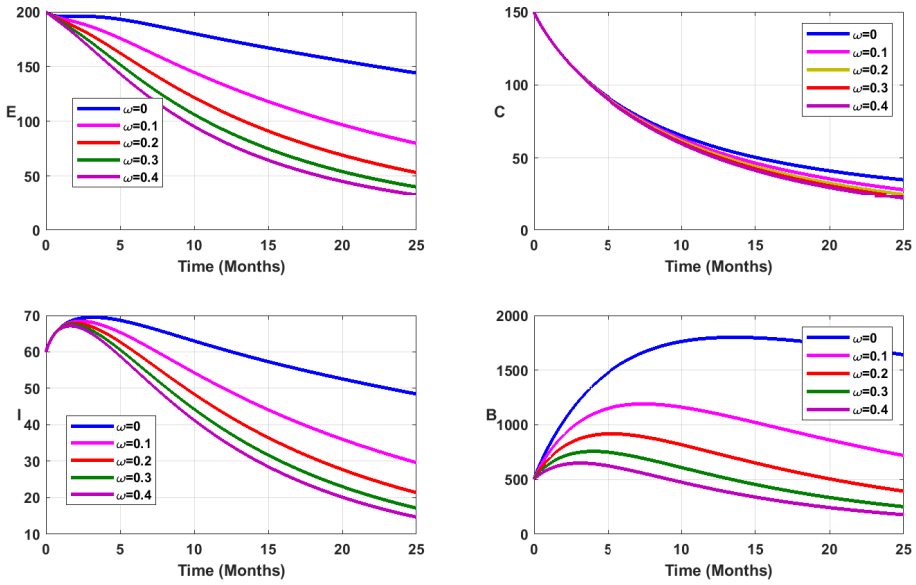

Figure 7. Simulation results showing the infected state variable profiles when vaccination is combined with environmental sanitation, for fractional order $\eta = 0.90$.

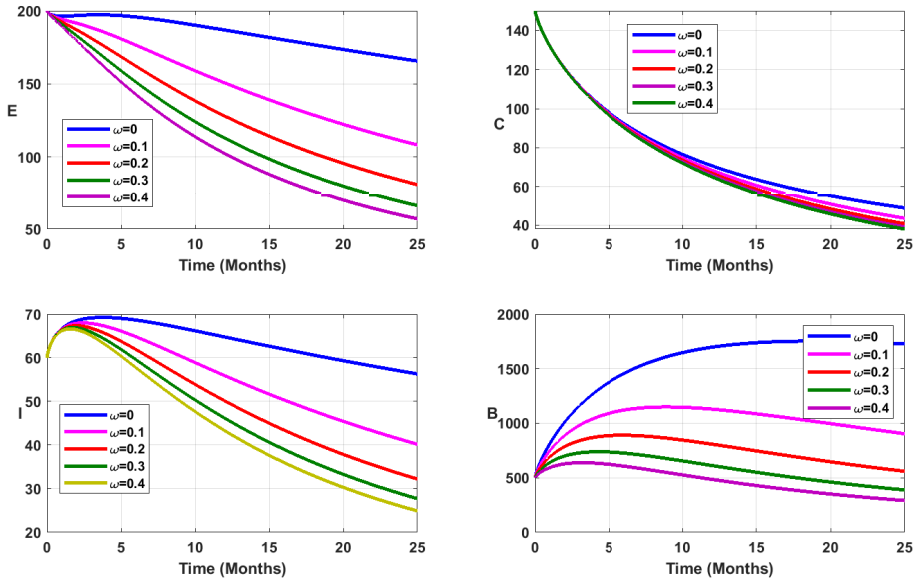

Figure 8. Simulation results showing the infected state variable profiles when vaccination is combined with environmental sanitation, for fractional order $\eta = 0.80$.

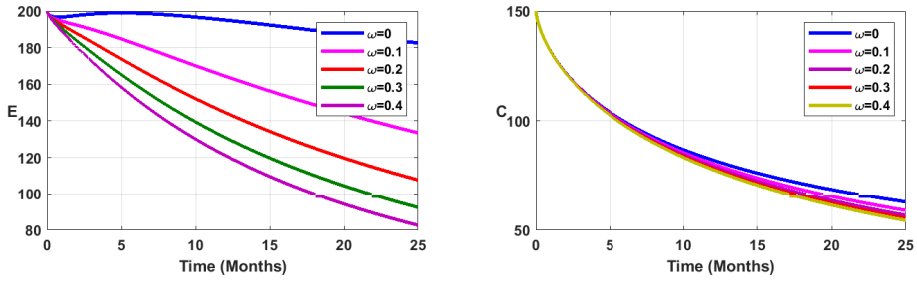

Figure 9. *Cont*.

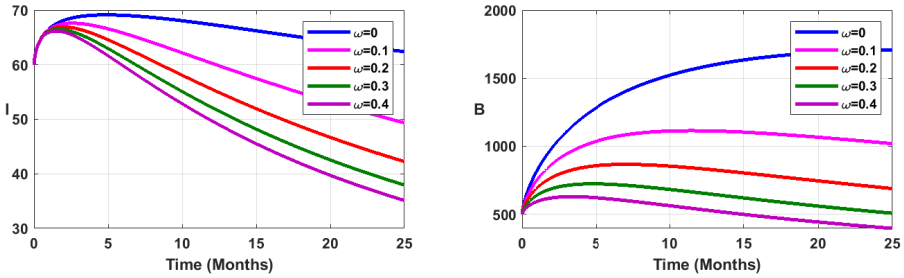

Figure 9. Simulation results showing the infected state variable profiles when vaccination is combined with environmental sanitation, for fractional order $\eta = 0.70$.

3.2. Numerical Results of the Fractional Model with Standard Incidence Law

To simulate the new fractional model (35), we use the parameter values listed in Table 2. Note that the new typhoid model has been calibrated using real data from Mbandjock, Cameroon (see [5,6]). In Figure 10, panel (a) shows the cumulative typhoid cases versus fitted confirmed cases (infectious individuals tested positive), which is equal to $(1-q)\gamma_1 E(t) + (1-p)\gamma_2 C(t)$, while panel (b) presents the cumulative estimated cases for the next year. The following fractions are used as initial conditions $S(0) = 20{,}950/32{,}000$, $V(0) = 20/32{,}000$, $E(0) = 200/32{,}000$, $C(0) = 150/32{,}000$, $I(0) = 60/32{,}000$, $R(0) = 1/32{,}000$, and $B(0) = 500/10^6$. The relative change is $r = 1.83 \times 10^{-7}$ and the function tolerance is equal to 10^{-6}.

Table 2. Estimated parameter values of the new typhoid model (35).

Parameter	Values	Source	Parameter	Values	Source
Λ_h	3	Fitted	μ_b	0.0015	Fitted
γ_1	0.1512	Fitted	ϵ	0.9497	Fitted
γ_2	0.3039	Fitted	ξ	0.1538	Fitted
δ	0.1382	Fitted	β	0.60	Fitted
ν	0.00050	Fitted	K	995.7957	Fitted
σ	0.4992	Fitted	$\mathcal{R}_{c\star}$	1.4348	Estimated

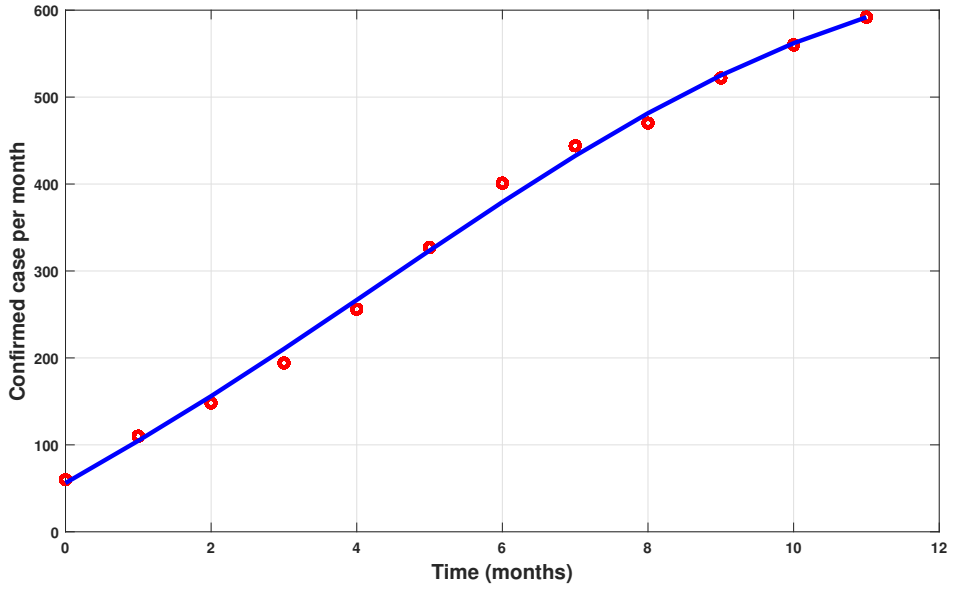

(**a**)

Figure 10. *Cont.*

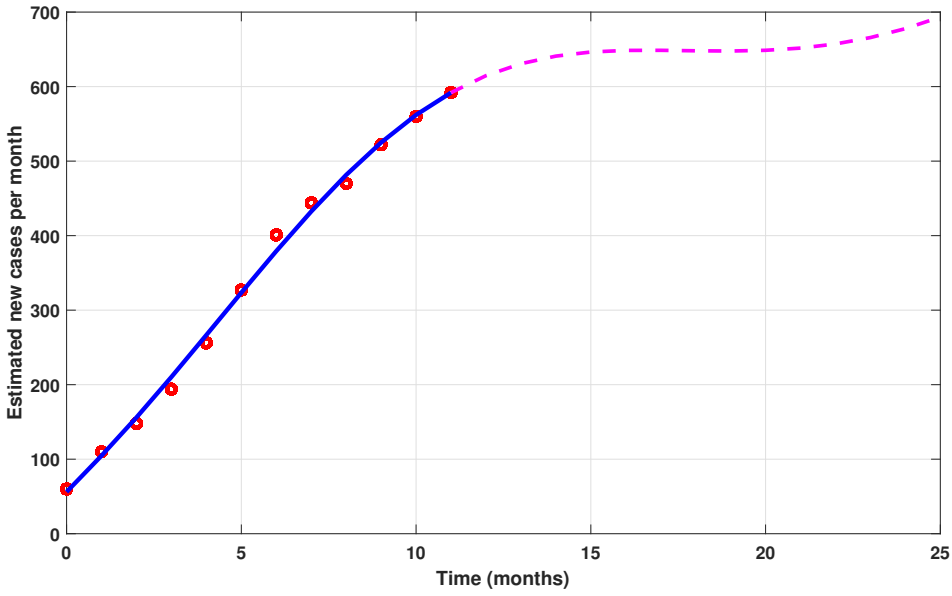

Figure 10. Parameter estimation and forecasting of cumulative new cases of typhoid fever in Mbandjock, Cameroon, from 1 July 2019 to 31 August 2020, for the new model (35). Red bullets denote real data (see [5,6]). The fitted model is represented with the blue line, and new forecasted cases are represented by the dotted line.

First, we observe the general dynamics of the new fractional model. The results are displayed in Figure 11. As for the case of the fractional model with mass incidence law (5), Figure 11 reveals that when the fractional order η decreases, the solutions of our fractional model (35) have different behaviors. The number of typhoid cases decreases and the peak is delayed when the fractional order decreases.

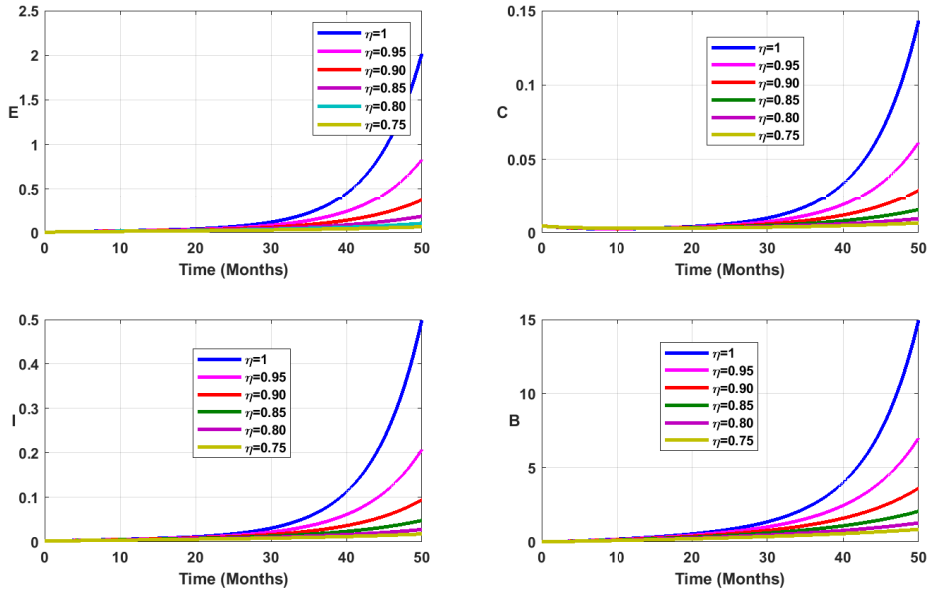

Figure 11. Simulation results showing the fractional dynamics on the infected state variable profiles for different values of the fractional-order parameter η.

Vaccination coverage impact is studied numerically. From Figures 12–15, it follows that the more ξ increases, the fewer individuals are infected. This shows that mass vaccination plays a important role in reducing the spread of the disease.

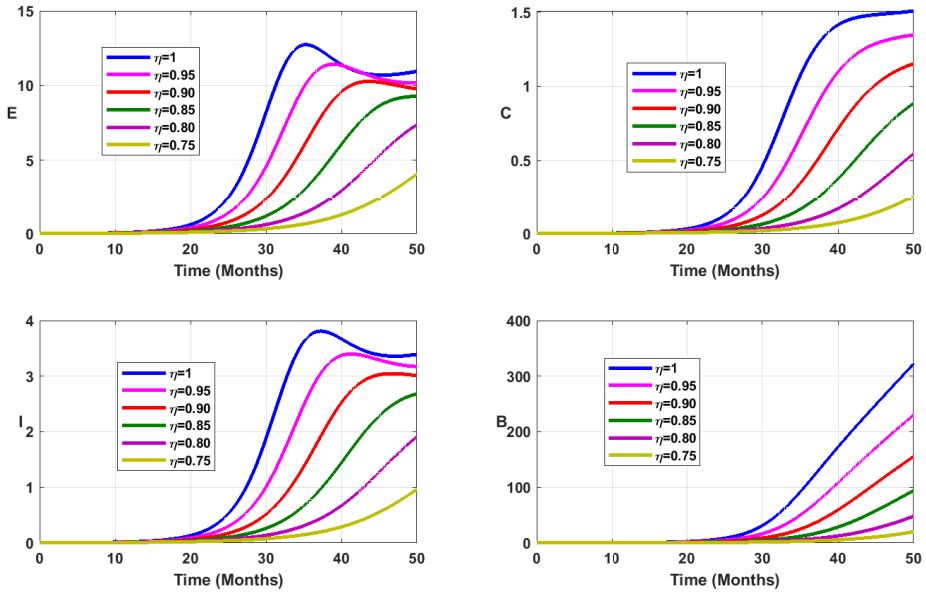

Figure 12. Simulation results showing the infected state variable profiles when the vaccination coverage $\xi = 0\%$ with different values of the fractional order.

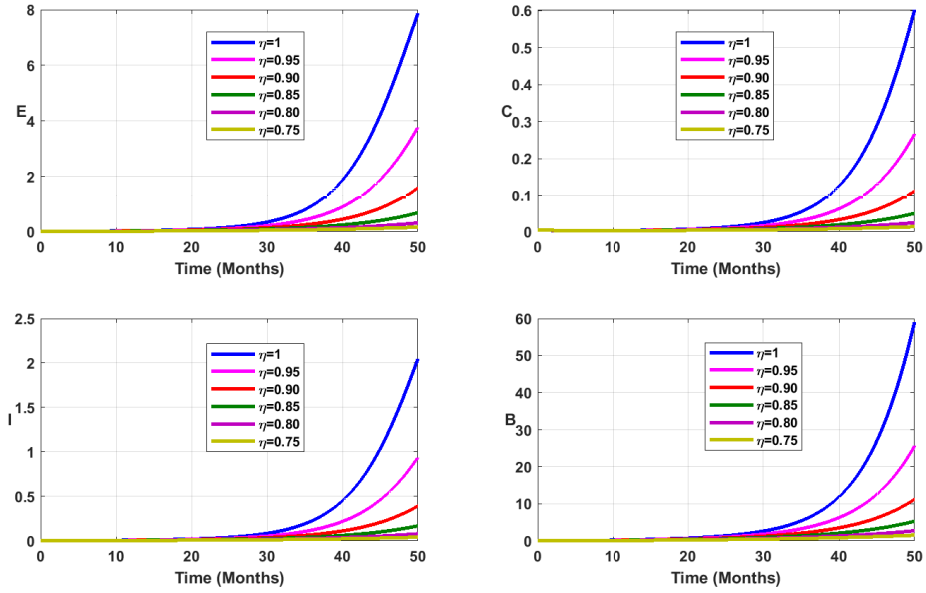

Figure 13. Simulation results showing the infected state variable profiles when the vaccination coverage $\xi = 20\%$ with different values of the fractional order.

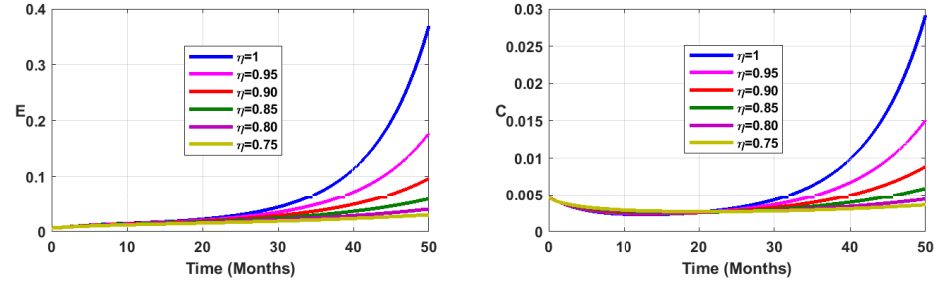

Figure 14. *Cont.*

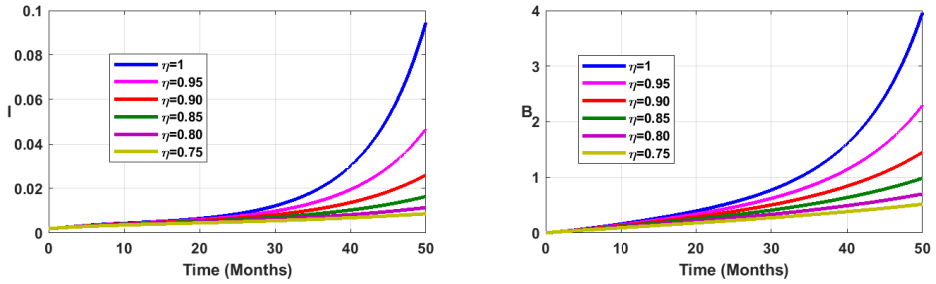

Figure 14. Simulation results showing the infected state variable profiles when the vaccination coverage $\xi = 50\%$ with different values of the fractional order.

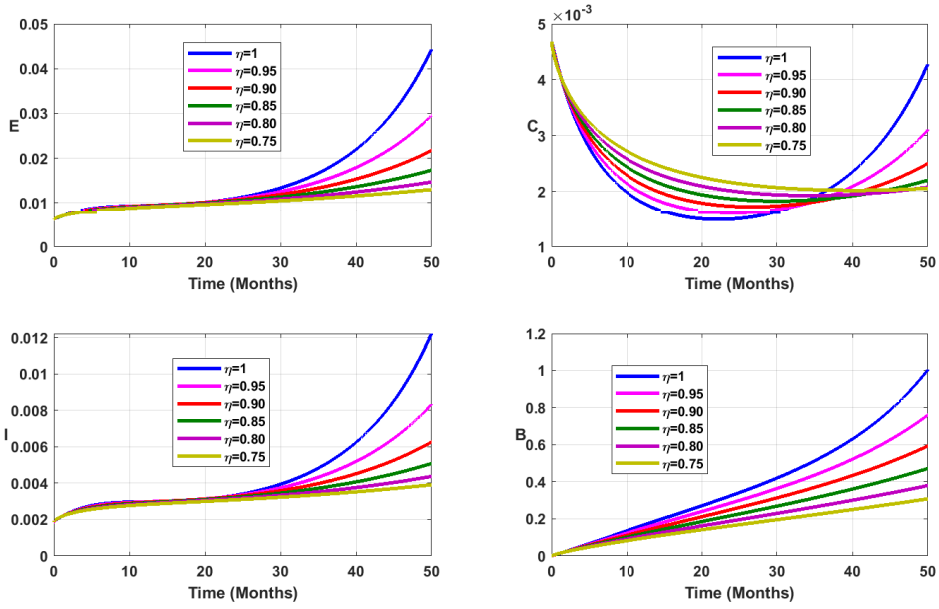

Figure 15. Simulation results showing the infected state variable profiles when the vaccination coverage $\xi = 90\%$ with different values of the fractional order.

4. Discussion and Conclusions

In this work, we extended our previous $SVEIR$-B compartmental model [5] by replacing the integer derivative with fractional derivatives, to evaluate the memory effect on the transmission dynamics of typhoid fever. We began by recalling some previous results on the integer model (the control reproduction number $\mathcal{R}_c$, existence and stability of equilibrium points). In order to describe the non-local character as well as long-term memory effects in the typhoid fever transmission dynamics, we replaced the integer derivative with the fractional derivative in the Caputo sense and studied the asymptotic stability of the disease-free equilibrium. Using fixed point theory, we proved the existence as well as the uniqueness of the solutions of the fractional model. We used the Adams–Bashforth method to construct the numerical scheme of the proposed fractional model. We then established the stability of this proposed numerical scheme. We simulated our fractional model using the Adams–Bashforth–Moulton scheme implemented by [39]. Using parameter values for Mbandjock, a city in the central region of Cameroon, we simulates the model by varying the fractional-order parameter, the vaccination coverage, and the bacterial decay rate. Apart from the fact that the solutions of the fractional model converged to the solutions of the integer model when the fractional-order approached one ($\eta = 1$), the simulation results showed that the expected date of the disease peak was forward delayed when the fractional-order parameter decreased. In addition, combining vaccination with environmental sanitation can permit a considerable reduction in the disease's spread.

We then extended the previous models by replacing the mass action incidence law with the standard incidence. The analysis of the models showed that the disease-free equilibrium is also globally asymptotically stable whenever the corresponding reproduction number $\mathcal{R}_{c\star}$ is less than one. Due to the complexity of the newly proposed models, we could not prove the existence and uniqueness of the endemic equilibrium. However, numerical simulations showed that it is possible that the new typhoid fever models permit a unique endemic equilibrium that is globally stable whenever $\mathcal{R}_{c\star} > 1$, and no equilibrium otherwise. We also found that, from a quantitative point of view, the disease burden was overestimated with the models the with mass incidence law compared to the one with the standard incidence law. Indeed, for the models with mass incidence, the control reproduction number was estimated at 2.4750, while the one with the standard incidence was estimated at 1.4348. This was in accordance with our previous work in which we considered the standard incidence law. In [6], the control reproduction number was estimated at 1.3722. As for the models with mass action incidences, we observed a delay in the disease peaks whenever the fractional-order derivative decreased.

It was observed that mass vaccination can overcome this disease. In fact, if the means are put in place to finance and implement vaccination campaigns in rural areas, it is possible to eradicate typhoid fever. Moreover, these vaccination campaigns must be accompanied by awareness campaigns among the population in order to combat this type of disease, as well as instructing citizens on ways to protect their environment against the proliferation of salmonella.

Our main contribution in this paper consisted in the formulation, using both integer and fractional derivatives, of new transmission dynamics typhoid fever models that incorporate the standard incidence rates and mass vaccination. The values of the control reproductive number differ from the model with mass action incidence and those with the standard incidences. Indeed, for the model with mass action incidences, $\mathcal{R}_c = 2.4750$, while, for those with standard incidences, $\mathcal{R}_{c*} = 1.4348$. This proves that mass action incidence overestimates the disease burden.

Author Contributions: Conceptualization, H.A. and R.K.R.; methodology, H.A. and R.K.R.; software, H.A. and R.K.R.; validation, H.A., R.K.R. and K.S.N.; formal analysis, H.A.; investigation, H.A. and R.K.R.; resources, H.A., R.K.R. and K.S.N.; data curation, H.A. and R.K.R.; writing—original draft preparation, H.A.; writing—review and editing, H.A., R.K.R. and K.S.N.; visualization, H.A.; supervision, H.A.; project administration, H.A.; funding acquisition, K.S.N. All authors have read and agreed to the published version of the manuscript.

Funding: The APC was funded by Kottakkaran Sooppy Nisar. No other funds have been received for this work.

Institutional Review Board Statement: Not applicable.

Informed Consent Statement: Not applicable.

Data Availability Statement: The data used to calibrate our model were taken from Mbandjock district hospital.

Acknowledgments: The authors thank the LESIA laboratory manager of the National School of Agro-industrial Sciences of the University of Ngaoundéré for their hospitality during the performance of the numerical simulations. The authors thank the Handling Editor and the anonymous reviewers for their comments and suggestions, which enabled us to improve the manuscript.

Conflicts of Interest: The authors declare no conflict of interest.

Appendix A. Proof of Proposition 3

Proof. The Jacobian matrix of (34) (resp. (35)) evaluated at the disease-free equilibrium $\mathcal{Q}_0$ is given by

$$\mathcal{J}(\mathcal{Q}_0) = \begin{pmatrix} -k_1 & \theta & 0 & -\frac{S_0\beta}{N_0} & -\frac{S_0\beta}{N_0} & \alpha & -\frac{S_0\nu}{K} \\ \xi & -k_2 & 0 & -\frac{\pi V_0\beta}{N_0} & -\frac{\pi V_0\beta}{N_0} & 0 & -\frac{\pi V_0\nu}{K} \\ 0 & 0 & -k_3 & \frac{H_0\beta}{N_0} & \frac{H_0\beta}{N_0} & 0 & \frac{H_0\nu}{K} \\ 0 & 0 & \gamma_1 q & -k_4 & 0 & 0 & 0 \\ 0 & 0 & q_1\gamma_1 & p_1\gamma_2 & -k_8 & 0 & 0 \\ 0 & 0 & 0 & p\gamma_2 & \sigma & -k_6 & 0 \\ 0 & 0 & 0 & p_c & p_i & 0 & -\mu_b \end{pmatrix} = \begin{pmatrix} \mathcal{J}_1 & \mathcal{J}_2 \\ \mathcal{J}_3 & \mathcal{J}_4 \end{pmatrix},$$

where $\mathcal{J}_1 = \begin{pmatrix} -k_1 & \theta \\ \xi & -k_2 \end{pmatrix}$, $\mathcal{J}_4 = \begin{pmatrix} -k_3 & \frac{H_0\beta}{N_0} & \frac{H_0\beta}{N_0} & 0 & \frac{H_0\nu}{K} \\ \gamma_1 q & -k_4 & 0 & 0 & 0 \\ q_1\gamma_1 & p_1\gamma_2 & -k_8 & 0 & 0 \\ 0 & p\gamma_2 & \sigma & -k_6 & 0 \\ 0 & p_c & p_i & 0 & -\mu_b \end{pmatrix}$,

$\mathcal{J}_2 = \begin{pmatrix} 0 & -\frac{S_0\beta}{N_0} & -\frac{S_0\beta}{N_0} & \alpha & -\frac{S_0\nu}{K} \\ 0 & -\frac{\pi V_0\beta}{N_0} & -\frac{\pi V_0\beta}{N_0} & 0 & -\frac{\pi V_0\nu}{K} \end{pmatrix}$, and $\mathcal{J}_3 = \mathbf{0}_{\mathbb{R}^{5\times 2}}$. The eigenvalues of $\mathcal{J}(\mathcal{Q}_0)$ are those of $\mathcal{J}_1$ and $\mathcal{J}_4$. It is evident that the eigenvalues of $\mathcal{J}_1$ have negative real parts. Indeed, the characteristic polynomial of $\mathcal{J}_1$ is $\mathcal{T}(x) = \det(\mathcal{J}_1 - xI_2) = x^2 + (k_1 + k_2)x + k_7$. Since all its coefficients are positive, it follows that all its roots have negative real parts. A trivial eigenvalue of $\mathcal{J}_4$ is $x = -k_6$. The others are the roots of the following polynomial: $\mathcal{I}(x) = x^4 + a_1x^3 + a_2x^2 + a_3x + a_4$, with $a_1 = \mu_b + k_8 + k_4 + k_3$, $a_4 = k_3k_4k_8\mu_b(1 - \mathcal{R}_c^\star)(\mathcal{R}_c^\star - R_1 + 1)$,

$$\begin{aligned} a_2 = \frac{1}{k_8q + p_1\gamma_2q + q_1k_4}\Big[&k_8^2\mu_bq + k_4k_8\mu_bq + k_3k_8\mu_bq + p_1\gamma_2k_8\mu_bq + p_1\gamma_2k_4\mu_bq + p_1\gamma_2k_3\mu_bq \\ &+k_4k_8^2q + k_3k_8^2q + k_3k_4k_8q(1 - R_1) + p_1\gamma_2k_4k_8q + p_1\gamma_2k_3k_8q + p_1\gamma_2k_3k_4q + q_1k_4k_8\mu_b \\ &+q_1k_4^2\mu_b + q_1k_3k_4\mu_b + q_1k_4^2k_8 + q_1k_3k_4k_8(1 - R_1) + q_1k_3k_4^2\Big], \end{aligned}$$

and

$$\begin{aligned} a_3 = &\frac{1}{((p_1\gamma_2k_8 + p_1^2\gamma_2^2)p_i + (k_8^2 + p_1\gamma_2k_8)p_c)q^2 + ((q_1k_4k_8 + 2p_1q_1\gamma_2k_4)p_i + q_1k_4k_8p_c)q + q_1^2k_4^2p_i}\times \\ &\times\Big[((((p_1\gamma_2k_4 + p_1\gamma_2k_3)k_8^2 + (((1 - R_1)p_1\gamma_2k_3 + p_1^2\gamma_2^2)k_4 + p_1^2\gamma_2^2k_3)k_8 + p_1^2\gamma_2^2k_3k_4)\mu_b \\ &+(1 - R_1)p_1\gamma_2k_3k_4k_8^2 + (1 - R_1)p_1^2\gamma_2^2k_3k_4k_8)p_i + \mathbf{K}_1p_c)q^2 \\ &+(\mathbf{K}_2p_i + (q_1k_3k_4^2k_8\mu_b\Big(1 - \mathcal{R}_{c\star}^2 + R_1\mathcal{R}_{c\star}\Big) + q_1k_4^2k_8^2\mu_b + (1 - R_1)q_1k_3k_4k_8^2\mu_b + (1 - R_1)q_1k_3k_4^2k_8^2)p_c)q \\ &+(q_1^2k_3k_4^2k_8\mu_b(1 - \mathcal{R}_{c\star})(1 - R_1 + \mathcal{R}_{c\star}) + q_1^2k_4^3k_8\mu_b + q_1^2k_3k_4^3\mu_b + (1 - R_1)q_1^2k_3k_4^3k_8)p_i\Big]. \end{aligned}$$

$$\begin{aligned} \mathbf{K}_1 = &\Big\{k_8(1 - \mathcal{R}_{c\star})(1 - R_1 + \mathcal{R}_{c\star}) + p_1\gamma_2\Big(1 - \mathcal{R}_{c\star}^2 + R_1\mathcal{R}_{c\star}\Big)\Big\}k_3k_4k_8\mu_b \\ &+ (k_4 + k_3)(k_8 + p_1\gamma_2)k_8^2\mu_b + (1 - R_1)(k_8 + p_1\gamma_2)k_3k_4k_8^2 \\ \mathbf{K}_2 = &(k_8 + p_1\gamma_2)q_1k_3k_4k_8\mu_b\Big(1 - \mathcal{R}_{c\star}^2 + R_1\mathcal{R}_{c\star}\Big) \\ &+ (1 - R_1)p_1\gamma_2q_1k_3k_4k_8\mu_b + ((1 - R_1)q_1k_3 + 2p_1\gamma_2q_1)k_4^2k_8\mu_b^2 + 2p_1\gamma_2q_1k_3k_4^2\mu_b \\ &+ q_1k_4^2k_8^2\mu_b + q_1k_3k_4^2k_8(1 - R_1)(k_8 + 2p_1\gamma_2) \end{aligned}$$

It is clear that a_1 is always positive, and a_i, $i \in \{2,3,4\}$ are positive if $\mathcal{R}_{c\star} < 1$. Indeed, it is important to note that

$$\mathcal{R}_{c\star} < 1 \Longrightarrow R_1 < 1, \tag{A1}$$

which implies that $\mathbf{K}_1 > 0$ and $\mathbf{K}_2 > 0$.

Thus, all coefficients of the polynomial $\mathcal{I}(x)$ are always positive whenever $\mathcal{R}_{c\star} < 1$. It follows that, if $\mathcal{R}_{c\star} < 1$, then the disease-free equilibrium is locally asymptotically stable if and only if the following conditions hold (because of the length of the expressions, we omit them here):

$$a_1 a_2 - a_3 > 0 \quad \text{and} \quad a_1 a_2 a_3 - a_1^2 a_4 - a_3^2 > 0. \tag{A2}$$

This ends the proof. □

It remains now to prove the corresponding result for the new fractional model (35). To this aim, let us define the following equation:

$$\det[r(I - (1-\eta)\mathcal{J}(\mathcal{Q}_0)) - \eta \mathcal{J}(\mathcal{Q}_0)] = 0, \tag{A3}$$

which is the characteristic equation of

$$\mathcal{J}(\mathcal{Q}_0) = \begin{pmatrix} -k_1 & \vartheta & 0 & -\frac{S_0\beta}{N_0} & -\frac{S_0\beta}{N_0} & 0 & -\frac{S_0\nu}{K} \\ \xi & -k_2 & 0 & -\frac{V_0\beta\pi}{N_0} & -\frac{V_0\beta\pi}{N_0} & 0 & -\frac{V_0\nu\pi}{N_0} \\ 0 & 0 & -k_3 & \frac{H_0\beta}{N_0} & \frac{H_0\beta}{N_0} & 0 & \frac{H_0\nu}{K} \\ 0 & 0 & \gamma_1 q & -k_4 & 0 & 0 & 0 \\ 0 & 0 & q_1\gamma_1 & p_1\gamma_2 & -k_8 & 0 & 0 \\ 0 & 0 & 0 & \gamma_2 p & \sigma & -k_6 & 0 \\ 0 & 0 & 0 & p_c & p_i & 0 & -\mu_b \end{pmatrix}.$$

From [4,30], it follows that $\mathcal{Q}_0$ is asymptotically stable, for the new fractional model, if all solutions of (A3) have negative real parts.

Setting $\mathcal{D} := [r(I - (1-\eta)\mathcal{J}(\mathcal{Q}_0)) - \eta \mathcal{Q}_0] = \begin{pmatrix} D_1 & \bullet \\ \mathbf{0}_{\mathbb{R}^{5\times 2}} & D_4 \end{pmatrix}$, with

$$D_1 := \begin{pmatrix} (\eta_1 k_1 + 1)r + k_1\eta & -\eta_1 r\vartheta - \eta\vartheta \\ -\eta_1 r\xi - \eta\xi & (\eta_1 k_2 + 1)r + k_2\eta \end{pmatrix} \text{ and}$$

$$D_4 := \begin{pmatrix} (\eta_1 k_3 + 1)r + k_3\eta & -\frac{H_0\eta_1\beta r}{N_0} - \frac{H_0\beta\eta}{N_0} & -\frac{H_0\eta_1\beta r}{N_0} - \frac{H_0\beta\eta}{N_0} & 0 & -\frac{H_0\eta_1\nu r}{K} - \frac{H_0\eta\nu}{K} \\ -\eta_1\gamma_1 qr - \gamma_1\eta q & (\eta_1 k_4 + 1)r + k_4\eta & 0 & 0 & 0 \\ -\eta_1 q_1\gamma_1 r - q_1\gamma_1\eta & -\eta_1 p_1\gamma_2 r - p_1\gamma_2\eta & (\eta_1 k_8 + 1)r + k_8\eta & 0 & 0 \\ 0 & -\eta_1\gamma_2 pr - \gamma_2\eta p & -\eta_1 r\sigma - \eta\sigma & (\eta_1 k_6 + 1)r + k_6\eta & 0 \\ 0 & -\eta_1 p_c r - p_c\eta & -\eta_1 p_i r - \eta p_i & 0 & (\eta_1\mu_b + 1)r + \mu_b\eta \end{pmatrix},$$

it follows that the solutions of (A3) are the solutions of $\det(D_1) = 0$ and $\det(D_4) = 0$. From the Proof of Theorem 2, it follows that the solutions of $\det(D_1) = 0$ have negative real parts. It thus remains to show that the same is true for $\det(D_4) = 0$. Note that $r = -\dfrac{k_8\eta}{\eta_1 k_8 + 1} < 0$ is a solution of $\det(D_4) = 0$. The others are the solutions of $\det(D_4^\star) = 0$, where

$$D_4^\star := \begin{pmatrix} (\eta_1 k_3 + 1)r + k_3\eta & -\frac{H_0\eta_1\beta r}{N_0} - \frac{H_0\beta\eta}{N_0} & -\frac{H_0\eta_1\beta r}{N_0} - \frac{H_0\beta\eta}{N_0} & -\frac{H_0\eta_1\nu r}{K} - \frac{H_0\eta\nu}{K} \\ -\eta_1\gamma_1 qr - \gamma_1\eta q & (\eta_1 k_4 + 1)r + k_4\eta & 0 & 0 \\ -\eta_1 q_1\gamma_1 r - q_1\gamma_1\eta & -\eta_1 p_1\gamma_2 r - p_1\gamma_2\eta & (\eta_1 k_8 + 1)r + k_8\eta & 0 \\ 0 & -\eta_1 p_c r - p_c\eta & -\eta_1 p_i r - \eta p_i & (\eta_1\mu_b + 1)r + \mu_b\eta \end{pmatrix}.$$

After some straightforward algebraic computations, we obtain that

$$\det(D_4^\star) = 0 \Longleftrightarrow r^4 + \frac{A_2}{A_1}r^3 + \frac{A_3}{A_1}r^2 + \frac{A_4}{A_1}r + \frac{A_5}{A_1} = 0, \tag{A4}$$

where

$$
\begin{aligned}
A_1 = {} & ((((-p_1\gamma_2k_3k_4k_8^2 - p_1^2\gamma_2^2k_3k_4k_8)\mu_b\mathcal{R}_{c\star}^2 + (R_1p_1\gamma_2k_3k_4k_8^2 + R_1p_1^2\gamma_2^2k_3k_4k_8)\mu_b\mathcal{R}_{c\star} \\
& + ((1-R_1)p_1\gamma_2k_3k_4k_8^2 + (1-R_1)p_1^2\gamma_2^2k_3k_4k_8)\mu_b)\eta^4 \\
& + (((p_1\gamma_2k_4 + p_1\gamma_2k_3)k_8^2 + (((1-R_1)p_1\gamma_2k_3 + p_1^2\gamma_2^2)k_4 + p_1^2\gamma_2^2k_3)k_8 + p_1^2\gamma_2^2k_3k_4)\mu_b \\
& + (1-R_1)p_1\gamma_2k_3k_4k_8^2 + (1-R_1)p_1^2\gamma_2^2k_3k_4k_8)\eta^3 + ((p_1\gamma_2k_8^2 + (p_1\gamma_2k_4 + p_1\gamma_2k_3 + p_1^2\gamma_2^2)k_8 + p_1^2\gamma_2^2k_4 + p_1^2\gamma_2^2k_3)\mu_b \\
& + (p_1\gamma_2k_4 + p_1\gamma_2k_3)k_8^2 + (((1-R_1)p_1\gamma_2k_3 + p_1^2\gamma_2^2)k_4 + p_1^2\gamma_2^2k_3)k_8 + p_1^2\gamma_2^2k_3k_4)\eta^2 \\
& + ((p_1\gamma_2k_8 + p_1^2\gamma_2^2)\mu_b + p_1\gamma_2k_8^2 + (p_1\gamma_2k_4 + p_1\gamma_2k_3 + p_1^2\gamma_2^2)k_8 + p_1^2\gamma_2^2k_4 + p_1^2\gamma_2^2k_3)\eta + p_1\gamma_2k_8 + p_1^2\gamma_2^2)p_i \\
& + ((-k_3k_4k_8^3 - p_1\gamma_2k_3k_4k_8^2)\mu_bR_c^2 + (R_1k_3k_4k_8^3 + R_1p_1\gamma_2k_3k_4k_8^2)\mu_b\mathcal{R}_{c\star} + ((1-R_1)k_3k_4k_8^3 + (1-R_1)p_1\gamma_2k_3k_4k_8^2)\mu_b)p_c\eta^4 \\
& + ((-k_3k_4k_8^2 - p_1\gamma_2k_3k_4k_8)\mu_b\mathcal{R}_{c\star}^2 + (R_1k_3k_4k_8^2 + R_1p_1\gamma_2k_3k_4k_8)\mu_b\mathcal{R}_{c\star} + ((k_4+k_3)k_8^3 + (((1-R_1)k_3 + p_1\gamma_2)k_4 + p_1\gamma_2k_3)k_8^2 \\
& + p_1\gamma_2k_3k_4k_8)\mu_b + (1-R_1)k_3k_4k_8^3 + (1-R_1)p_1\gamma_2k_3k_4k_8^2)p_c\eta^3 + ((k_8^3 + (k_4+k_3+p_1\gamma_2)k_8^2 + (p_1\gamma_2k_4 + p_1\gamma_2k_3)k_8)\mu_b \\
& + (k_4+k_3)k_8^3 + (((1-R_1)k_3 + p_1\gamma_2)k_4 + p_1\gamma_2k_3)k_8^2 + p_1\gamma_2k_3k_4k_8)p_c\eta^2 + ((k_8^2 + p_1\gamma_2k_8)\mu_b + k_8^3 + (k_4+k_3+p_1\gamma_2)k_8^2 \\
& + (p_1\gamma_2k_4 + p_1\gamma_2k_3)k_8)p_c\eta + (k_8^2 + p_1\gamma_2k_8)p_c)q^2 \\
& + ((((-q_1k_3k_4^2k_8^2 - 2p_1q_1\gamma_2k_3k_4^2k_8)\mu_b\mathcal{R}_{c\star}^2 + (R_1q_1k_3k_4^2k_8^2 + 2R_1p_1q_1\gamma_2k_3k_4^2k_8)\mu_b\mathcal{R}_{c\star} \\
& + ((1-R_1)q_1k_3k_4^2k_8^2 + (2-2R_1)p_1q_1\gamma_2k_3k_4^2k_8)\mu_b)\eta^4 \\
& + ((-q_1k_3k_4k_8^2 - p_1q_1\gamma_2k_3k_4k_8)\mu_b\mathcal{R}_{c\star}^2 + (R_1q_1k_3k_4k_8^2 + R_1p_1q_1\gamma_2k_3k_4k_8)\mu_b\mathcal{R}_{c\star} \\
& + ((q_1k_4^2 + q_1k_3k_4)k_8^2 + (((1-R_1)q_1k_3 + 2p_1q_1\gamma_2)k_4^2 + (2-R_1)p_1q_1\gamma_2k_3k_4)k_8 + 2p_1q_1\gamma_2k_3k_4^2)\mu_b \\
& + (1-R_1)q_1k_3k_4^2k_8^2 + (2-2R_1)p_1q_1\gamma_2k_3k_4^2k_8)\eta^3 + ((q_1k_4k_8^2 + (q_1k_4^2 + (q_1k_3 + 2p_1q_1\gamma_2)k_4)k_8 + 2p_1q_1\gamma_2k_4^2 + 2p_1q_1\gamma_2k_3k_4)\mu_b \\
& + (q_1k_4^2 + q_1k_3k_4)k_8^2 + (((1-R_1)q_1k_3 + 2p_1q_1\gamma_2)k_4^2 + (2-R_1)p_1q_1\gamma_2k_3k_4)k_8 + 2p_1q_1\gamma_2k_3k_4^2)\eta^2 + ((q_1k_4k_8 + 2p_1q_1\gamma_2k_4)\mu_b \\
& + q_1k_4k_8^2 + (q_1k_4^2 + (q_1k_3 + 2p_1q_1\gamma_2)k_4)k_8 + 2p_1q_1\gamma_2k_4^2 + 2p_1q_1\gamma_2k_3k_4)\eta + q_1k_4k_8 + 2p_1q_1\gamma_2k_4)p_i \\
& + (-q_1k_3k_4^2k_8^2\mu_b\mathcal{R}_{c\star}^2 + R_1q_1k_3k_4^2k_8^2\mu_b\mathcal{R}_{c\star} + (1-R_1)q_1k_3k_4^2k_8^2\mu_b)p_c\eta^4 \\
& + (-q_1k_3k_4^2k_8\mu_b\mathcal{R}_{c\star}^2 + R_1q_1k_3k_4^2k_8\mu_b\mathcal{R}_{c\star} + ((q_1k_4^2 + (1-R_1)q_1k_3k_4)k_8^2 + q_1k_3k_4^2k_8)\mu_b + (1-R_1)q_1k_3k_4^2k_8^2)p_c\eta^3 \\
& + ((q_1k_4k_8^2 + (q_1k_4^2 + q_1k_3k_4)k_8)\mu_b + (q_1k_4^2 + (1-R_1)q_1k_3k_4)k_8^2 + q_1k_3k_4^2k_8)p_c\eta^2 \\
& + (q_1k_4k_8\mu_b + q_1k_4k_8^2 + (q_1k_4^2 + q_1k_3k_4)k_8)p_c\eta + q_1k_4k_8p_c)q \\
& + ((-q_1^2k_3k_4^3k_8\mu_b\mathcal{R}_{c\star}^2 + R_1q_1^2k_3k_4^3k_8\mu_b\mathcal{R}_{c\star} + (1-R_1)q_1^2k_3k_4^3k_8\mu_b)\eta^4 \\
& + (-q_1^2k_3k_4^2k_8\mu_b\mathcal{R}_{c\star}^2 + R_1q_1^2k_3k_4^2k_8\mu_b\mathcal{R}_{c\star} + ((q_1^2k_4^3 + (1-R_1)q_1^2k_3k_4^2)k_8 + q_1^2k_3k_4^3)\mu_b + (1-R_1)q_1^2k_3k_4^3k_8)\eta^3 \\
& + ((q_1^2k_4^2k_8 + q_1^2k_4^3 + q_1^2k_3k_4^2)\mu_b + (q_1^2k_4^3 + (1-R_1)q_1^2k_3k_4^2)k_8 + q_1^2k_3k_4^3)\eta^2 + (q_1^2k_4^2\mu_b + q_1^2k_4^2k_8 + q_1^2k_4^3 + q_1^2k_3k_4^2)\eta + q_1^2k_4^2)p_i,
\end{aligned}
$$

$$
\begin{aligned}
A_4 = {} & ((4(k_8 + p_1\gamma_2)p_1\gamma_2k_3k_4k_8\mu_b(1-\mathcal{R}_{c\star})(1+\mathcal{R}_{c\star}-R_1)\eta^4 \\
& + (((p_1\gamma_2k_4 + p_1\gamma_2k_3)k_8^2 + (((1-R_1)p_1\gamma_2k_3 + p_1^2\gamma_2^2)k_4 + p_1^2\gamma_2^2k_3)k_8 + p_1^2\gamma_2^2k_3k_4)\mu_b \\
& + (1-R_1)p_1\gamma_2k_3k_4k_8^2 + (1-R_1)p_1^2\gamma_2^2k_3k_4k_8)\eta^3)p_i + 4(k_8 + p_1\gamma_2)(1-\mathcal{R}_{c\star})(1+\mathcal{R}_{c\star}-R_1)k_3k_4k_8^2\mu_bp_c\eta^4 \\
& + ((k_8 + p_1\gamma_2)k_3k_4k_8\mu_b\mathcal{R}_{c\star}(R_1 - \mathcal{R}_{c\star}) + ((k_4+k_3)k_8^3 \\
& + (((1-R_1)k_3 + p_1\gamma_2)k_4 + p_1\gamma_2k_3)k_8^2 + p_1\gamma_2k_3k_4k_8)\mu_b + (1-R_1)k_3k_4k_8^3 + (1-R_1)p_1\gamma_2k_3k_4k_8^2)p_c\eta^3)q^2 \\
& + ((((-4q_1k_3k_4^2k_8^2 - 8p_1q_1\gamma_2k_3k_4^2k_8)\mu_b\mathcal{R}_{c\star}^2 + (4R_1q_1k_3k_4^2k_8^2 + 8R_1p_1q_1\gamma_2k_3k_4^2k_8)\mu_b\mathcal{R}_{c\star} \\
& + ((4-4R_1)q_1k_3k_4^2k_8^2 + (8-8R_1)p_1q_1\gamma_2k_3k_4^2k_8)\mu_b)\eta^4 \\
& + ((-q_1k_3k_4k_8^2 - p_1q_1\gamma_2k_3k_4k_8)\mu_b\mathcal{R}_{c\star}^2 + (R_1q_1k_3k_4k_8^2 + R_1p_1q_1\gamma_2k_3k_4k_8)\mu_b\mathcal{R}_{c\star} + ((q_1k_4^2 + q_1k_3k_4)k_8^2 \\
& + (((1-R_1)q_1k_3 + 2p_1q_1\gamma_2)k_4^2 + (2-R_1)p_1q_1\gamma_2k_3k_4)k_8 + 2p_1q_1\gamma_2k_3k_4^2)\mu_b + (1-R_1)q_1k_3k_4^2k_8^2 \\
& + (2-2R_1)p_1q_1\gamma_2k_3k_4^2k_8)\eta^3)p_i + (-4q_1k_3k_4^2k_8^2\mu_b\mathcal{R}_{c\star}^2 + 4R_1q_1k_3k_4^2k_8^2\mu_b\mathcal{R}_{c\star} + (4-4R_1)q_1k_3k_4^2k_8^2\mu_b)p_c\eta^4 \\
& + (-q_1k_3k_4^2k_8\mu_b\mathcal{R}_{c\star}^2 + R_1q_1k_3k_4^2k_8\mu_b\mathcal{R}_{c\star} + ((q_1k_4^2 + (1-R_1)q_1k_3k_4)k_8^2 + q_1k_3k_4^2k_8)\mu_b \\
& + (1-R_1)q_1k_3k_4^2k_8^2)p_c\eta^3)q + ((-4q_1^2k_3k_4^3k_8\mu_b\mathcal{R}_{c\star}^2 + 4R_1q_1^2k_3k_4^3k_8\mu_b\mathcal{R}_{c\star} + (4-4R_1)q_1^2k_3k_4^3k_8\mu_b)\eta^4 \\
& + (-q_1^2k_3k_4^2k_8\mu_b\mathcal{R}_{c\star}^2 + R_1q_1^2k_3k_4^2k_8\mu_b\mathcal{R}_{c\star} + ((q_1^2k_4^3 + (1-R_1)q_1^2k_3k_4^2)k_8 + q_1^2k_3k_4^3)\mu_b + (1-R_1)q_1^2k_3k_4^3k_8)\eta^3)p_i,
\end{aligned}
$$

$$A_5 = k_3k_4k_8\mu_b(\mathcal{R}_{c\star} - R_1 + 1)\eta^4(k_8q + p_1\gamma_2q + q_1k_4)(p_1\gamma_2p_iq + k_8p_cq + q_1k_4p_i)(1 - \mathcal{R}_{c\star}),$$

$$\begin{aligned}
A_2 = {} & ((((-4p_1\gamma_2k_3k_4k_8^2 - 4p_1^2\gamma_2^2k_3k_4k_8)\mu_b\mathcal{R}_{c\star}^2 + (4R_1p_1\gamma_2k_3k_4k_8^2 + 4R_1p_1^2\gamma_2^2k_3k_4k_8)\mu_b\mathcal{R}_{c\star} \\
& + ((4 - 4R_1)p_1\gamma_2k_3k_4k_8^2 + (4 - 4R_1)p_1^2\gamma_2^2k_3k_4k_8)\mu_b)\eta^4 \\
& + (((3p_1\gamma_2k_4 + 3p_1\gamma_2k_3)k_8^2 + (((3 - 3R_1)p_1\gamma_2k_3 + 3p_1^2\gamma_2^2)k_4 + 3p_1^2\gamma_2^2k_3)k_8 + 3p_1^2\gamma_2^2k_3k_4)\mu_b \\
& + (3 - 3R_1)p_1\gamma_2k_3k_4k_8^2 + (3 - 3R_1)p_1^2\gamma_2^2k_3k_4k_8)\eta^3 + ((2p_1\gamma_2k_8^2 + (2p_1\gamma_2k_4 + 2p_1\gamma_2k_3 + 2p_1^2\gamma_2^2)k_8 + 2p_1^2\gamma_2^2k_4 + 2p_1^2\gamma_2^2k_3)\mu_b \\
& + (2p_1\gamma_2k_4 + 2p_1\gamma_2k_3)k_8^2 + (((2 - 2R_1)p_1\gamma_2k_3 + 2p_1^2\gamma_2^2)k_4 + 2p_1^2\gamma_2^2k_3)k_8 + 2p_1^2\gamma_2^2k_3k_4)\eta^2 \\
& + ((p_1\gamma_2k_8 + p_1^2\gamma_2^2)\mu_b + p_1\gamma_2k_8^2 + (p_1\gamma_2k_4 + p_1\gamma_2k_3 + p_1^2\gamma_2^2)k_8 + p_1^2\gamma_2^2k_4 + p_1^2\gamma_2^2k_3)\eta)p_i \\
& + ((-4k_3k_4k_8^3 - 4p_1\gamma_2k_3k_4k_8^2)\mu_b\mathcal{R}_{c\star}^2 + (4R_1k_3k_4k_8^3 + 4R_1p_1\gamma_2k_3k_4k_8^2)\mu_b\mathcal{R}_{c\star} + 4(1 - R_1)(k_8 + p_1\gamma_2)k_3k_4k_8^2\mu_b)p_c\eta^4 \\
& + ((-3k_3k_4k_8^2 - 3p_1\gamma_2k_3k_4k_8)\mu_b\mathcal{R}_{c\star}^2 + (3R_1k_3k_4k_8^2 + 3R_1p_1\gamma_2k_3k_4k_8)\mu_b\mathcal{R}_{c\star} \\
& + (3(k_4 + k_3)k_8^3 + ((3(1 - R_1)k_3 + 3p_1\gamma_2)k_4 + 3p_1\gamma_2k_3)k_8^2 + 3p_1\gamma_2k_3k_4k_8)\mu_b + 3(1 - R_1)k_3k_4k_8^3 + 3(1 - R_1)p_1\gamma_2k_3k_4k_8^2)p_c\eta^3 \\
& + ((2k_8^3 + (2k_4 + 2k_3 + 2p_1\gamma_2)k_8^2 + (2p_1\gamma_2k_4 + 2p_1\gamma_2k_3)k_8)\mu_b + (2k_4 + 2k_3)k_8^3 + (((2 - 2R_1)k_3 + 2p_1\gamma_2)k_4 + 2p_1\gamma_2k_3)k_8^2 \\
& + 2p_1\gamma_2k_3k_4k_8)p_c\eta^2 + ((k_8^2 + p_1\gamma_2k_8)\mu_b + k_8^3 + (k_4 + k_3 + p_1\gamma_2)k_8^2 + (p_1\gamma_2k_4 + p_1\gamma_2k_3)k_8)p_c\eta)q^2 \\
& + ((((-4q_1k_3k_4^2k_8^2 - 8p_1q_1\gamma_2k_3k_4^2k_8)\mu_b\mathcal{R}_{c\star}^2 + (4R_1q_1k_3k_4^2k_8^2 + 8R_1p_1q_1\gamma_2k_3k_4^2k_8)\mu_b\mathcal{R}_{c\star} \\
& + ((4 - 4R_1)q_1k_3k_4^2k_8^2 + (8 - 8R_1)p_1q_1\gamma_2k_3k_4^2k_8)\mu_b)\eta^4 \\
& + ((-3q_1k_3k_4k_8^2 - 3p_1q_1\gamma_2k_3k_4k_8)\mu_b\mathcal{R}_{c\star}^2 + (3R_1q_1k_3k_4k_8^2 + 3R_1p_1q_1\gamma_2k_3k_4k_8)\mu_b\mathcal{R}_{c\star} \\
& + ((3q_1k_4^2 + 3q_1k_3k_4)k_8^2 + (((3 - 3R_1)q_1k_3 + 6p_1q_1\gamma_2)k_4^2 + (6 - 3R_1)p_1q_1\gamma_2k_3k_4)k_8 + 6p_1q_1\gamma_2k_3k_4^2)\mu_b + (3 - 3R_1)q_1k_3k_4^2k_8^2 \\
& + (6 - 6R_1)p_1q_1\gamma_2k_3k_4^2k_8)\eta^3 + ((2q_1k_4k_8^2 + (2q_1k_4^2 + (2q_1k_3 + 4p_1q_1\gamma_2)k_4)k_8 + 4p_1q_1\gamma_2k_4^2 + 4p_1q_1\gamma_2k_3k_4)\mu_b \\
& + (2q_1k_4^2 + 2q_1k_3k_4)k_8^2 + (((2 - 2R_1)q_1k_3 + 4p_1q_1\gamma_2)k_4^2 + (4 - 2R_1)p_1q_1\gamma_2k_3k_4)k_8 + 4p_1q_1\gamma_2k_3k_4^2)\eta^2 \\
& + ((q_1k_4k_8 + 2p_1q_1\gamma_2k_4)\mu_b + q_1k_4k_8^2 + (q_1k_4^2 + (q_1k_3 + 2p_1q_1\gamma_2)k_4)k_8 + 2p_1q_1\gamma_2k_4^2 + 2p_1q_1\gamma_2k_3k_4)\eta)p_i \\
& + 4(1 - R_1 + R_1\mathcal{R}_{c\star} - \mathcal{R}_{c\star}^2)q_1k_3k_4^2k_8^2\mu_bp_c\eta^4 \\
& + (-3q_1k_3k_4^2k_8\mu_b\mathcal{R}_{c\star}^2 + 3R_1q_1k_3k_4^2k_8\mu_b\mathcal{R}_{c\star} + ((3q_1k_4^2 + (3 - 3R_1)q_1k_3k_4)k_8^2 + 3q_1k_3k_4^2k_8)\mu_b + (3 - 3R_1)q_1k_3k_4^2k_8^2)p_c\eta^3 \\
& + ((2q_1k_4k_8^2 + (2q_1k_4^2 + 2q_1k_3k_4)k_8)\mu_b + (2q_1k_4^2 + (2 - 2R_1)q_1k_3k_4)k_8^2 + 2q_1k_3k_4^2k_8)p_c\eta^2 \\
& + (q_1k_4k_8\mu_b + q_1k_4k_8^2 + (q_1k_4^2 + q_1k_3k_4)k_8)p_c\eta)q \\
& + ((-4q_1^2k_3k_4^3k_8\mu_b\mathcal{R}_{c\star}^2 + 4R_1q_1^2k_3k_4^3k_8\mu_b\mathcal{R}_{c\star} + (4 - 4R_1)q_1^2k_3k_4^3k_8\mu_b)\eta^4 \\
& + (-3q_1^2k_3k_4^2k_8\mu_bR_c^2 + 3R_1q_1^2k_3k_4^2k_8\mu_b\mathcal{R}_{c\star} + ((3q_1^2k_4^3 + (3 - 3R_1)q_1^2k_3k_4^2)k_8 + 3q_1^2k_3k_4^3)\mu_b + (3 - 3R_1)q_1^2k_3k_4^3k_8)\eta^3 \\
& + ((2q_1^2k_4^2k_8 + 2q_1^2k_4^3 + 2q_1^2k_3k_4^2)\mu_b + (2q_1^2k_4^3 + (2 - 2R_1)q_1^2k_3k_4^2)k_8 + 2q_1^2k_3k_4^3)\eta^2 + (q_1^2k_4^2\mu_b + q_1^2k_4^2k_8 + q_1^2k_4^3 + q_1^2k_3k_4^2)\eta)p_i,
\end{aligned}$$

$$
\begin{aligned}
A_3 = {} & ((((-6p_1\gamma_2k_3k_4k_8^2 - 6p_1^2\gamma_2^2k_3k_4k_8)\mu_bR_c^2 + (6R_1p_1\gamma_2k_3k_4k_8^2 + 6R_1p_1^2\gamma_2^2k_3k_4k_8)\mu_bR_c \\
& + ((6-6R_1)p_1\gamma_2k_3k_4k_8^2 + (6-6R_1)p_1^2\gamma_2^2k_3k_4k_8)\mu_b)\eta^4 + (((3p_1\gamma_2k_4 + 3p_1\gamma_2k_3)k_8^2 \\
& + (((3-3R_1)p_1\gamma_2k_3 + 3p_1^2\gamma_2^2)k_4 + 3p_1^2\gamma_2^2k_3)k_8 + 3p_1^2\gamma_2^2k_3k_4)\mu_b + (3-3R_1)p_1\gamma_2k_3k_4k_8^2 + (3-3R_1)p_1^2\gamma_2^2k_3k_4k_8)\eta^3 \\
& + ((p_1\gamma_2k_8^2 + (p_1\gamma_2k_4 + p_1\gamma_2k_3 + p_1^2\gamma_2^2)k_8 + p_1^2\gamma_2^2k_4 + p_1^2\gamma_2^2k_3)\mu_b + (p_1\gamma_2k_4 + p_1\gamma_2k_3)k_8^2 \\
& + (((1-R_1)p_1\gamma_2k_3 + p_1^2\gamma_2^2)k_4 + p_1^2\gamma_2^2k_3)k_8 + p_1^2\gamma_2^2k_3k_4)\eta^2)p_i \\
& + ((-6k_3k_4k_8^3 - 6p_1\gamma_2k_3k_4k_8^2)\mu_b\mathcal{R}_{c\star}^2 + (6R_1k_3k_4k_8^3 + 6R_1p_1\gamma_2k_3k_4k_8^2)\mu_b\mathcal{R}_{c\star} + (6-6R_1)(k_3k_4k_8^3 + p_1\gamma_2k_3k_4k_8^2)\mu_b)p_c\eta^4 \\
& + ((-3k_3k_4k_8^2 - 3p_1\gamma_2k_3k_4k_8)\mu_b\mathcal{R}_{c\star}^2 + (3R_1k_3k_4k_8^2 + 3R_1p_1\gamma_2k_3k_4k_8)\mu_bR_c \\
& + ((3k_4+3k_3)k_8^3 + (((3-3R_1)k_3 + 3p_1\gamma_2)k_4 + 3p_1\gamma_2k_3)k_8^2 + 3p_1\gamma_2k_3k_4k_8)\mu_b + 3(1-R_1)k_3k_4k_8^2(k_8 + p_1\gamma_2))p_c\eta^3 \\
& + ((k_8^3 + (k_4+k_3+p_1\gamma_2)k_8^2 + p_1\gamma_2(k_4+k_3)k_8)\mu_b + (k_4+k_3)k_8^3 + (((1-R_1)k_3 + p_1\gamma_2)k_4 + p_1\gamma_2k_3)k_8^2 + p_1\gamma_2k_3k_4k_8)p_c\eta^2)q^2 \\
& + ((((-6q_1k_3k_4^2k_8^2 - 12p_1q_1\gamma_2k_3k_4^2k_8)\mu_bR_c^2 + (6R_1q_1k_3k_4^2k_8^2 + 12R_1p_1q_1\gamma_2k_3k_4^2k_8)\mu_b\mathcal{R}_{c\star} \\
& + ((6-6R_1)q_1k_3k_4^2k_8^2 + (12-12R_1)p_1q_1\gamma_2k_3k_4^2k_8)\mu_b)\eta^4 \\
& + ((-3q_1k_3k_4k_8^2 - 3p_1q_1\gamma_2k_3k_4k_8)\mu_b\mathcal{R}_{c\star}^2 + (3R_1q_1k_3k_4k_8^2 + 3R_1p_1q_1\gamma_2k_3k_4k_8)\mu_bR_c \\
& + ((3q_1k_4^2 + 3q_1k_3k_4)k_8^2 + (((3-3R_1)q_1k_3 + 6p_1q_1\gamma_2)k_4^2 + (6-3R_1)p_1q_1\gamma_2k_3k_4)k_8 + 6p_1q_1\gamma_2k_3k_4^2)\mu_b \\
& + (3-3R_1)q_1k_3k_4^2k_8^2 + (6-6R_1)p_1q_1\gamma_2k_3k_4^2k_8)\eta^3 \\
& + ((q_1k_4k_8^2 + (q_1k_4^2 + (q_1k_3 + 2p_1q_1\gamma_2)k_4)k_8 + 2p_1q_1\gamma_2k_4^2 + 2p_1q_1\gamma_2k_3k_4)\mu_b + (q_1k_4^2 + q_1k_3k_4)k_8^2 \\
& + (((1-R_1)q_1k_3 + 2p_1q_1\gamma_2)k_4^2 + (2-R_1)p_1q_1\gamma_2k_3k_4)k_8 + 2p_1q_1\gamma_2k_3k_4^2)\eta^2)p_i \\
& + (-6q_1k_3k_4^2k_8^2\mu_b\mathcal{R}_{c\star}^2 + 6R_1q_1k_3k_4^2k_8^2\mu_b\mathcal{R}_{c\star} + (6-6R_1)q_1k_3k_4^2k_8^2\mu_b)p_c\eta^4 \\
& + (-3q_1k_3k_4^2k_8\mu_b\mathcal{R}_{c\star}^2 + 3R_1q_1k_3k_4^2k_8\mu_b\mathcal{R}_{c\star} + ((3q_1k_4^2 + (3-3R_1)q_1k_3k_4)k_8^2 + 3q_1k_3k_4^2k_8)\mu_b + (3-3R_1)q_1k_3k_4^2k_8^2)p_c\eta^3 \\
& + ((q_1k_4k_8^2 + (q_1k_4^2 + q_1k_3k_4)k_8)\mu_b + (q_1k_4^2 + (1-R_1)q_1k_3k_4)k_8^2 + q_1k_3k_4^2k_8)p_c\eta^2)q \\
& + ((-6q_1^2k_3k_4^3k_8\mu_b\mathcal{R}_{c\star}^2 + 6R_1q_1^2k_3k_4^3k_8\mu_b\mathcal{R}_{c\star} + (6-6R_1)q_1^2k_3k_4^3k_8\mu_b)\eta^4 \\
& + (-3q_1^2k_3k_4^2k_8\mu_b\mathcal{R}_{c\star}^2 + 3R_1q_1^2k_3k_4^2k_8\mu_b\mathcal{R}_{c\star} + ((3q_1^2k_4^3 + (3-3R_1)q_1^2k_3k_4^2)k_8 + 3q_1^2k_3k_4^3)\mu_b + (3-3R_1)q_1^2k_3k_4^3k_8)\eta^3 \\
& + ((q_1^2k_4^2k_8 + q_1^2k_4^3 + q_1^2k_3k_4^2)\mu_b + (q_1^2k_4^3 + (1-R_1)q_1^2k_3k_4^2)k_8 + q_1^2k_3k_4^3)\eta^2)p_i.
\end{aligned}
$$

It is possible to show that all the above coefficients are positive whenever $\mathcal{R}_{c\star} < 1$. Then, it follows that, if $\mathcal{R}_c < 1$, then the disease-free equilibrium $\mathcal{Q}_0$ is asymptotically stable whenever the following Routh–Hurwitz criteria, $\frac{A_1A_2}{A_5^2} - \frac{A_3}{A_5} > 0$ and $\frac{A_1A_2A_3}{A_5^3} - \frac{A_1^2A_4}{A_5^3} - \frac{A_3^2}{A_5^2} > 0$, are satisfied for polynomial $\det(D_4^\star)$. (Given the heaviness of these coefficients, we do not present the Routh–Hurwitz conditions here.)

Appendix B. Proof of Theorem 6

Let us rewrite system (34) as

$$
\begin{pmatrix} \frac{dE}{dt} \\ \frac{dC}{dt} \\ \frac{dI}{dt} \\ \frac{dB}{dt} \end{pmatrix} = \begin{pmatrix} -k_3 & \frac{H_0\beta}{N_0} & \frac{H_0\beta}{N_0} & \frac{H_0\nu}{K} \\ \gamma_1 q & -k_4 & 0 & 0 \\ q_1\gamma_1 & p_1\gamma_2 & -k_8 & 0 \\ 0 & p_c & p_i & -\mu_b \end{pmatrix} \begin{pmatrix} E \\ C \\ I \\ B \end{pmatrix} - \mathcal{N}(S,V,E,C,I,R,B), \tag{A5}
$$

where $\mathcal{N}(S,V,E,C,I,R,B) = \begin{pmatrix} \beta(C+I)\left(\frac{H_0}{N_0} - \frac{H}{N}\right) + \nu B\left(\frac{H_0}{K} - \frac{H}{K+B}\right) \\ 0 \\ 0 \\ 0 \end{pmatrix}$.

In $\mathcal{W}$, $H = S + \pi V < H_0 = S_0 + \pi V_0$ for $t > 0$; thus, $\mathcal{N}(S, V, E, C, I, R, B) \geq \mathbf{O}_{\mathbb{R}^4}$. Note that Proposition 3 ensures that the following matrix

$$\mathcal{J}(\mathcal{Q}_0) = \begin{pmatrix} -k_3 & \frac{H_0\beta}{N_0} & \frac{H_0\beta}{N_0} & \frac{H_0\nu}{K} \\ \gamma_1 q & -k_4 & 0 & 0 \\ q_1\gamma_1 & p_1\gamma_2 & -k_8 & 0 \\ 0 & p_c & p_i & -\mu_b \end{pmatrix}$$

has all its eigenvalues with negative real parts. It follows that from the comparison theorem [40], $(E, C, I, B) \longrightarrow (0, 0, 0, 0)$ and $(S, V, R) \longrightarrow (S_0, V_0, 0)$ as $t \longrightarrow +\infty$. Thus, $(S, V, E, C, I, R, B) \longrightarrow \mathcal{Q}_0 = (S_0, V_0, 0, 0, 0, 0, 0)$ as $t \longrightarrow +\infty$. We finally conclude that the disease–free equilibrium is globally asymptotically stable in $\mathcal{W}$ if $\mathcal{R}_{c\star} < 1$.

References

1. World Health Organization. Typhoid vaccines: WHO position paper. *Wkly. Epidemiol. Rec.* **2008**, *83*, 49–59.
2. World Health Organization. Typhoid vaccines: WHO position paper–March 2018–Vaccins antityphoïdiques: Note de synthèse de l'OMS–mars 2018. *Wkly. Epidemiol. Rec.* **2018**, *93*, 153–172.
3. Ross, R. Some quantitative studies in epidemiology. *Nature* **1911**, *87*, 466–467. [CrossRef]
4. Abboubakar, H.; Kumar, P.; Erturk, V.S.; Kumar, A. A mathematical study of a tuberculosis model with fractional derivatives. *Int. J. Model. Simul. Sci. Comput.* **2021**, *12*, 2150037. [CrossRef]
5. Abboubakar, H.; Racke, R. Mathematical modeling, forecasting, and optimal control of typhoid fever transmission dynamics. *Chaos Solitons Fractals* **2021**, *149*, 111074. [CrossRef]
6. Abboubakar, H.; Kombou, L.K.; Koko, A.D.; Fouda, H.P.E.; Kumar, A. Projections and fractional dynamics of the typhoid fever: A case study of Mbandjock in the Centre Region of Cameroon. *Chaos Solitons Fractals* **2021**, *150*, 111129. [CrossRef]
7. Edward, S.; Nyerere, N. Modelling typhoid fever with education, vaccination and treatment. *Eng. Math.* **2016**, *1*, 44–52.
8. Mushayabasa, S. Modeling the impact of optimal screening on typhoid dynamics. *Int. J. Dyn. Control* **2016**, *4*, 330–338. [CrossRef]
9. Peter, O.J.; Ibrahim, M.O.; Edogbanya, H.O.; Oguntolu, F.A.; Oshinubi, K.; Ibrahim, A.A.; Ayoola, T.A.; Lawal, J.O. Direct and Indirect Transmission of Typhoid Fever Model with Optimal Control. *Results Phys.* **2021**, *27*, 104463. [CrossRef]
10. Tilahun, G.T.; Makinde, O.D.; Malonza, D. Modelling and optimal control of typhoid fever disease with cost-effective strategies. *Comput. Math. Methods Med.* **2017**, *2017*, 2324518. [CrossRef]
11. Tilahun, G.T.; Makinde, O.D.; Malonza, D. Co-dynamics of pneumonia and typhoid fever diseases with cost effective optimal control analysis. *Appl. Math. Comput.* **2018**, *316*, 438–459. [CrossRef]
12. Shaikh, A.S.; Nisar, K.S. Transmission dynamics of fractional order Typhoid fever model using Caputo–Fabrizio operator. *Chaos Solitons Fractals* **2019**, *128*, 355–365. [CrossRef]
13. Erturk, V.S.; Kumar, P. Solution of a COVID-19 model via new generalized Caputo-type fractional derivatives. *Chaos Solitons Fractals* **2020**, *139*, 110280. [CrossRef]
14. Kumar, P.; Erturk, V.S. Environmental persistence influences infection dynamics for a butterfly pathogen via new generalised Caputo type fractional derivative. *Chaos Solitons Fractals* **2021**, *144*, 110672. [CrossRef]
15. Kumar, P.; Erturk, V.S.; Almusawa, H. Mathematical structure of mosaic disease using microbial biostimulants via Caputo and Atangana–Baleanu derivatives. *Results Phys.* **2021**, *24*, 104186. [CrossRef]
16. Kumar, P.; Suat Ertürk, V.; Nisar, K.S. Fractional dynamics of huanglongbing transmission within a citrus tree. *Math. Methods Appl. Sci.* **2021**, *44*, 11404–11424. [CrossRef]
17. Kumar, P.; Erturk, V.S.; Murillo-Arcila, M. A complex fractional mathematical modeling for the love story of Layla and Majnun. *Chaos Solitons Fractals* **2021**, *150*, 111091. [CrossRef]
18. Loverro, A. *Fractional Calculus: History, Definitions and Applications for the Engineer*; Rapport Technique; Department of Aerospace and Mechanical Engineering, Univeristy of Notre Dame: Notre Dame, IN, USA, 2004; pp. 1–28.
19. Nabi, K.N.; Abboubakar, H.; Kumar, P. Forecasting of COVID-19 pandemic: From integer derivatives to fractional derivatives. *Chaos Solitons Fractals* **2020**, *141*, 110283. [CrossRef] [PubMed]
20. Angstmann, C.N.; Jacobs, B.A.; Henry, B.I.; Xu, Z. Intrinsic Discontinuities in Solutions of Evolution Equations Involving Fractional Caputo–Fabrizio and Atangana–Baleanu Operators. *Mathematics* **2020**, *8*, 2023. [CrossRef]
21. Tarasov, V.E. On chain rule for fractional derivatives. *Commun. Nonlinear Sci. Numer. Simul.* **2016**, *30*, 1–4. [CrossRef]
22. Tarasov, V.E. No violation of the Leibniz rule. No fractional derivative. *Commun. Nonlinear Sci. Numer. Simul.* **2013**, *18*, 2945–2948. [CrossRef]
23. Peter, O.; Ibrahim, M.; Oguntolu, F.; Akinduko, O.; Akinyemi, S. Direct and indirect transmission dynamics of typhoid fever model by differential transform method. *ATBU J. Sci. Technol. Educ. (JOSTE)* **2018**, *6*, 167–177.
24. Diethelm, K. An algorithm for the numerical solution of differential equations of fractional order. *Electron. Trans. Numer. Anal* **1997**, *5*, 1–6.
25. Diethelm, K.; Ford, N.J. Analysis of fractional differential equations. *J. Math. Anal. Appl.* **2002**, *265*, 229–248. [CrossRef]

26. Boccaletti, S.; Ditto, W.; Mindlin, G.; Atangana, A. Modeling and forecasting of epidemic spreading: The case of Covid-19 and beyond. *Chaos Solitons Fractals* **2020**, *135*, 109794. [CrossRef]
27. Khan, M.A.; Atangana, A.; Alzahrani, E. The dynamics of COVID-19 with quarantined and isolation. *Adv. Differ. Equ.* **2020**, *2020*, 425. [CrossRef]
28. Schmidt, A.; Gaul, L. On the numerical evaluation of fractional derivatives in multi-degree-of-freedom systems. *Signal Process.* **2006**, *86*, 2592–2601. [CrossRef]
29. van den Driessche, P.; Watmough, J. Reproduction numbers and the sub-threshold endemic equilibria for compartmental models of disease transmission. *Math. Biosci.* **2002**, *180*, 29–48. [CrossRef]
30. Li, H.; Cheng, J.; Li, H.B.; Zhong, S.M. Stability analysis of a fractional-order linear system described by the Caputo–Fabrizio derivative. *Mathematics* **2019**, *7*, 200. [CrossRef]
31. Wojtak, W.; Silva, C.J.; Torres, D.F. Uniform asymptotic stability of a fractional tuberculosis model. *Math. Model. Nat. Phenom.* **2018**, *13*, 9. [CrossRef]
32. Li, C.; Zeng, F. The finite difference methods for fractional ordinary differential equations. *Numer. Funct. Anal. Optim.* **2013**, *34*, 149–179. [CrossRef]
33. Diethelm, K.; Luchko, Y. Numerical solution of linear multi-term initial value problems of fractional order. *J. Comput. Anal. Appl.* **2004**, *6*, 243–263.
34. Diethelm, K.; Ford, N.J.; Freed, A.D. A predictor-corrector approach for the numerical solution of fractional differential equations. *Nonlinear Dyn.* **2002**, *29*, 3–22. [CrossRef]
35. Pieskä, J.; Laitinen, E.; Lapin, A. Predictor-corrector methods for solving continuous casting problem. In *Domain Decomposition Methods in Science and Engineering*; Springer: Berlin/Heidelberg, Germany, 2005; pp. 677–684.
36. Butcher, J.C. Numerical methods for ordinary differential equations in the 20th century. *J. Comput. Appl. Math.* **2000**, *125*, 1–29. [CrossRef]
37. Li, C.; Tao, C. On the fractional Adams method. *Comput. Math. Appl.* **2009**, *58*, 1573–1588. [CrossRef]
38. Abboubakar, H.; Kumar, P.; Rangaig, N.A.; Kumar, S. A Malaria Model with Caputo-Fabrizio and Atangana-Baleanu Derivatives. *Int. J. Model. Simul. Sci. Comput.* **2021**, *12*, 2150013. [CrossRef]
39. Garrappa, R. Predictor-Corrector PECE Method for Fractional Differential Equations. MATLAB, Central File Exchange [File ID: 32918]. Available online: https://www.mathworks.com/matlabcentral/fileexchange/32918-predictor-corrector-pece-method-for-fractional-differential-equations (accessed on 23 September 2021).
40. Lakshmikantham, V.; Leela, S.; Martynyuk, A.A. *Stability Analysis of Non Linear Systems*; Springer: Berlin/Heidelberg, Germany, 1989.